Gamma ray analysis and GW follow-up observations

Masaki Mori, Yoichi Asaoka, Shoji Torii,
Daisuke Zenita, Nick Cannady, Mike Cherry,
Yuta Kawakubo
for the CALET collaboration

CALET TIM at CNR-IFAC, Florence, February 04-06-27, 2020

Cannady et al., ApJS 238:5 (2018)

Gamma Ray Event Selection

= Electron Selection Cut + Gamma-ray ID Cut w/ Lower Energy Extension

100 GeV Event Examples

gamma-ray	electron	proton
Charge Z=0	Charge Z=1	

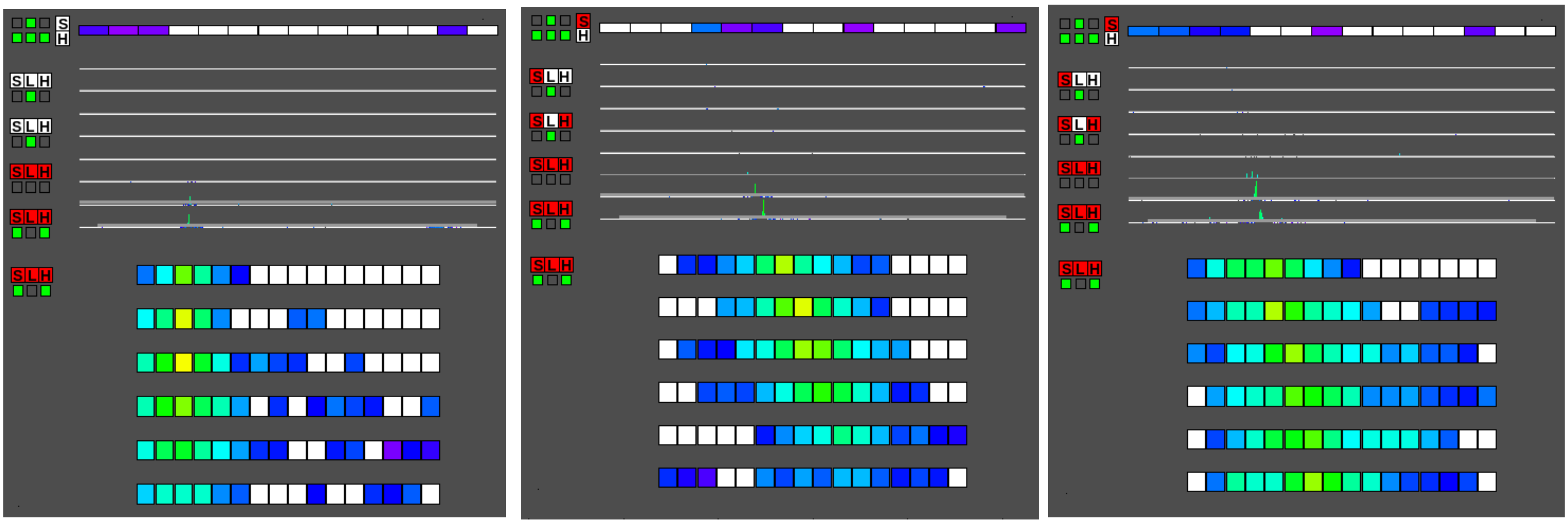

Electromagnetic Shower		Hadron Shower
well contained, constant shower development		larger spread

Mori, Asaoka et al., ICRC2019

Gamma-ray skymap

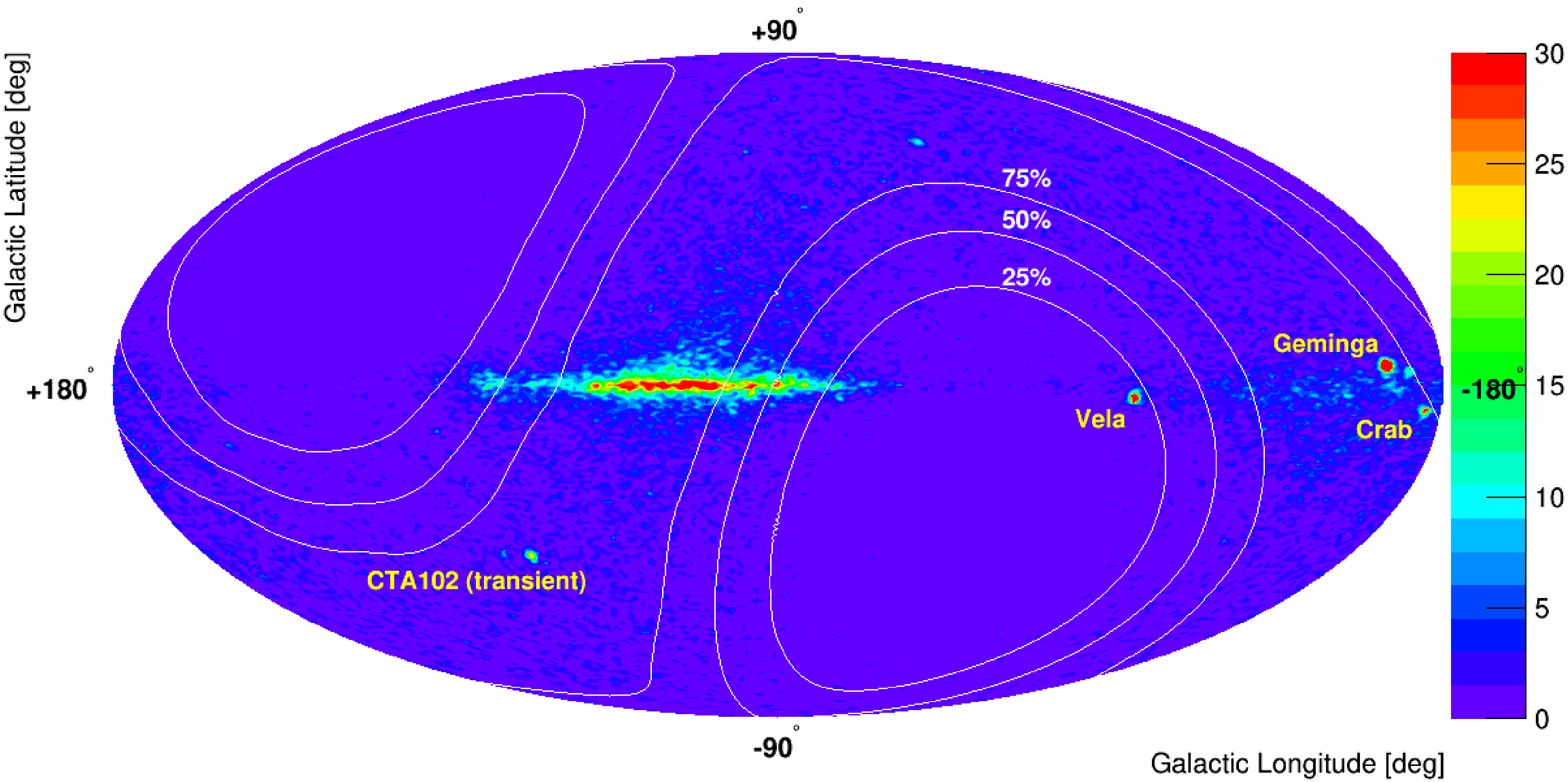

LE-γ mode, from 2015 November to 2018 May
(Contours show relative exposures)

Mori, Asaoka et al., ICRC2019+

Gamma-ray spectra

LE-γ mode
from 2015 November to 2018 May

"On-plane": $|l| < 80°$ & $|b| < 8°$, "Off-plane": $|b| > 8°$

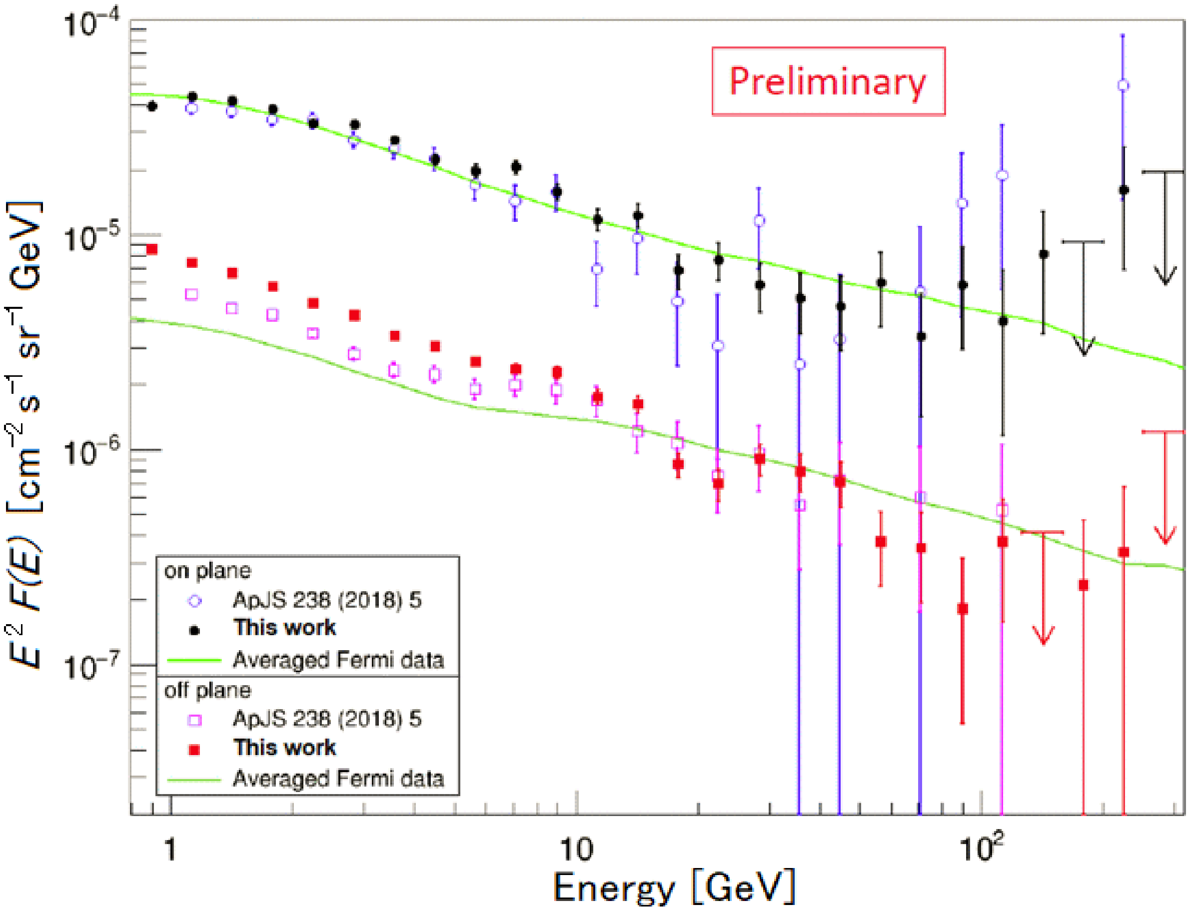

By Zenita

CTA 102 (AGN) light curve

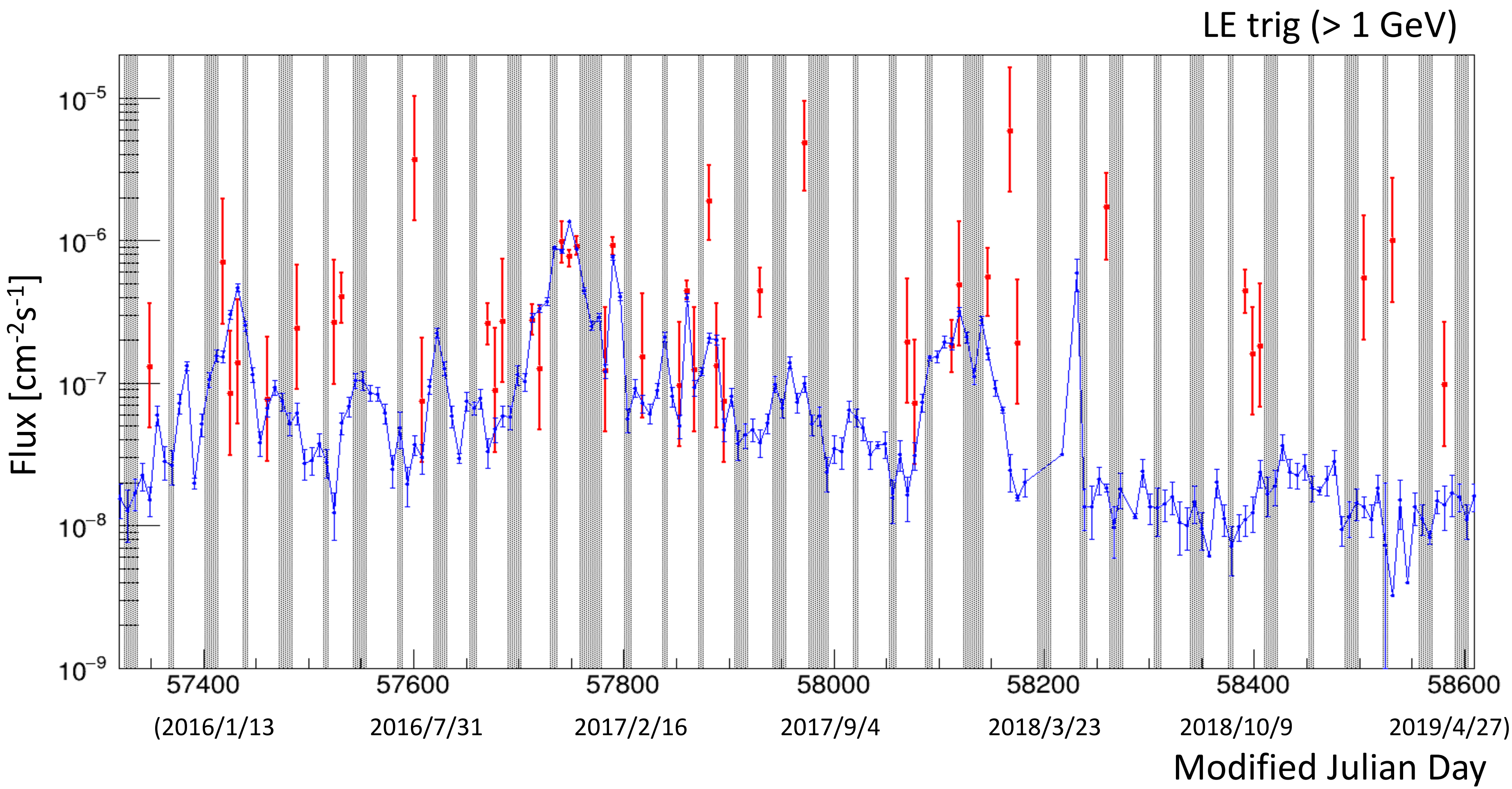

Red: CALET signal, Hatched: CALET upper limit ($<10^{-7} cm^{-2} s^{-1}$)

Blue: Fermi-LAT

By Zenita

CTA 102 (AGN) light curve

[Flare period]

LE trig (> 1 GeV)

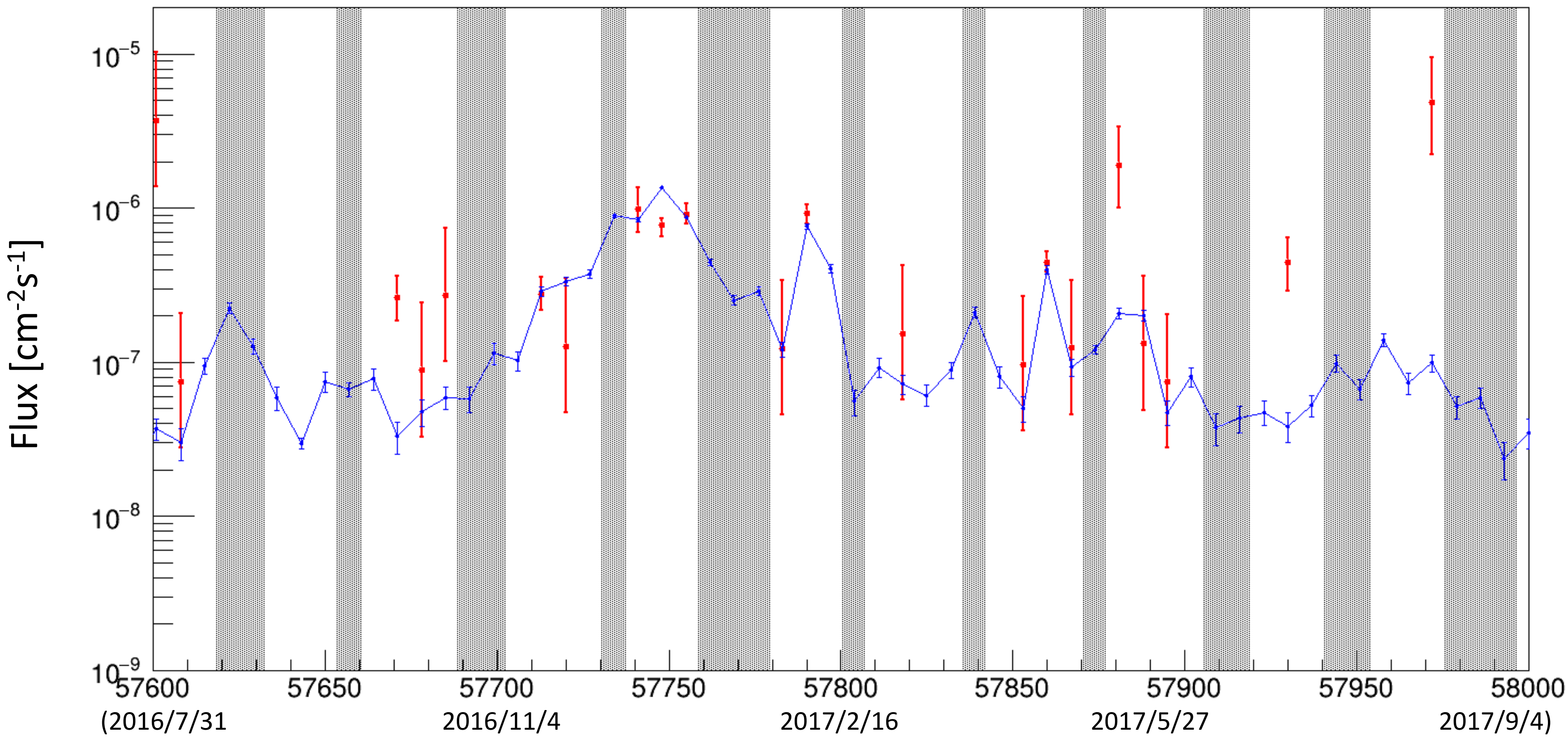

Red: CALET signal, Hatched: CALET upper limit (<10^{-7}cm^{-2}s^{-1})

Blue: Fermi-LAT

Toward higher energies
- Gamma-ray line? -

No result yet…

Gamma-ray lines from DM annihilation

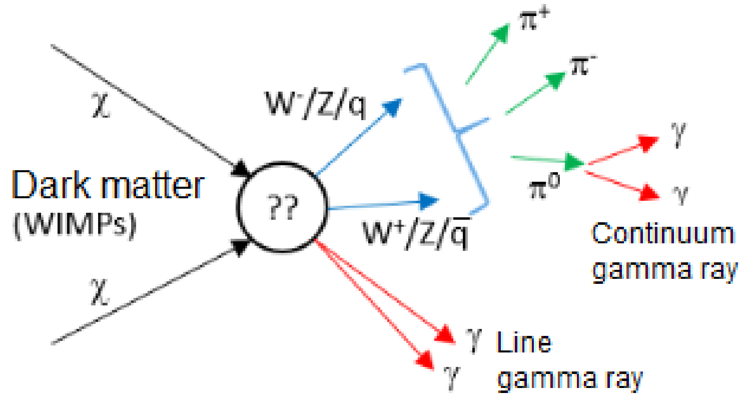

Neutralino

Kaluza-Klein

Bringmann and Calor 2013

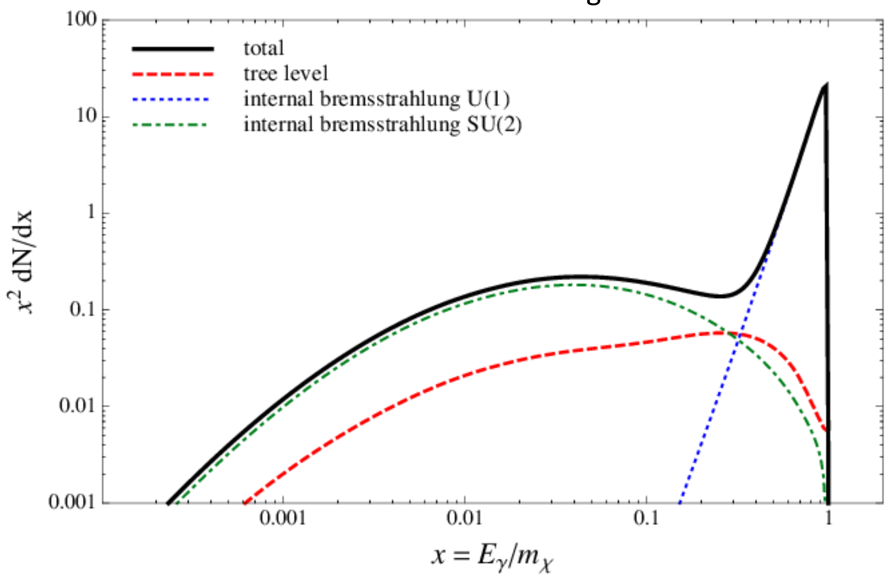

(loop suppressed – low branching ratio)

Tsuchida and Mori 2017

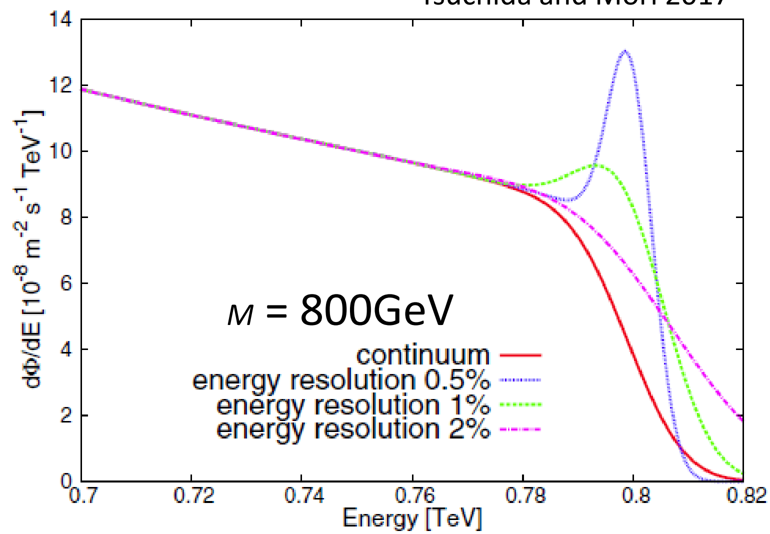

Limits by indirect searches

F. S. Queiroz, arXiv:1605.08788

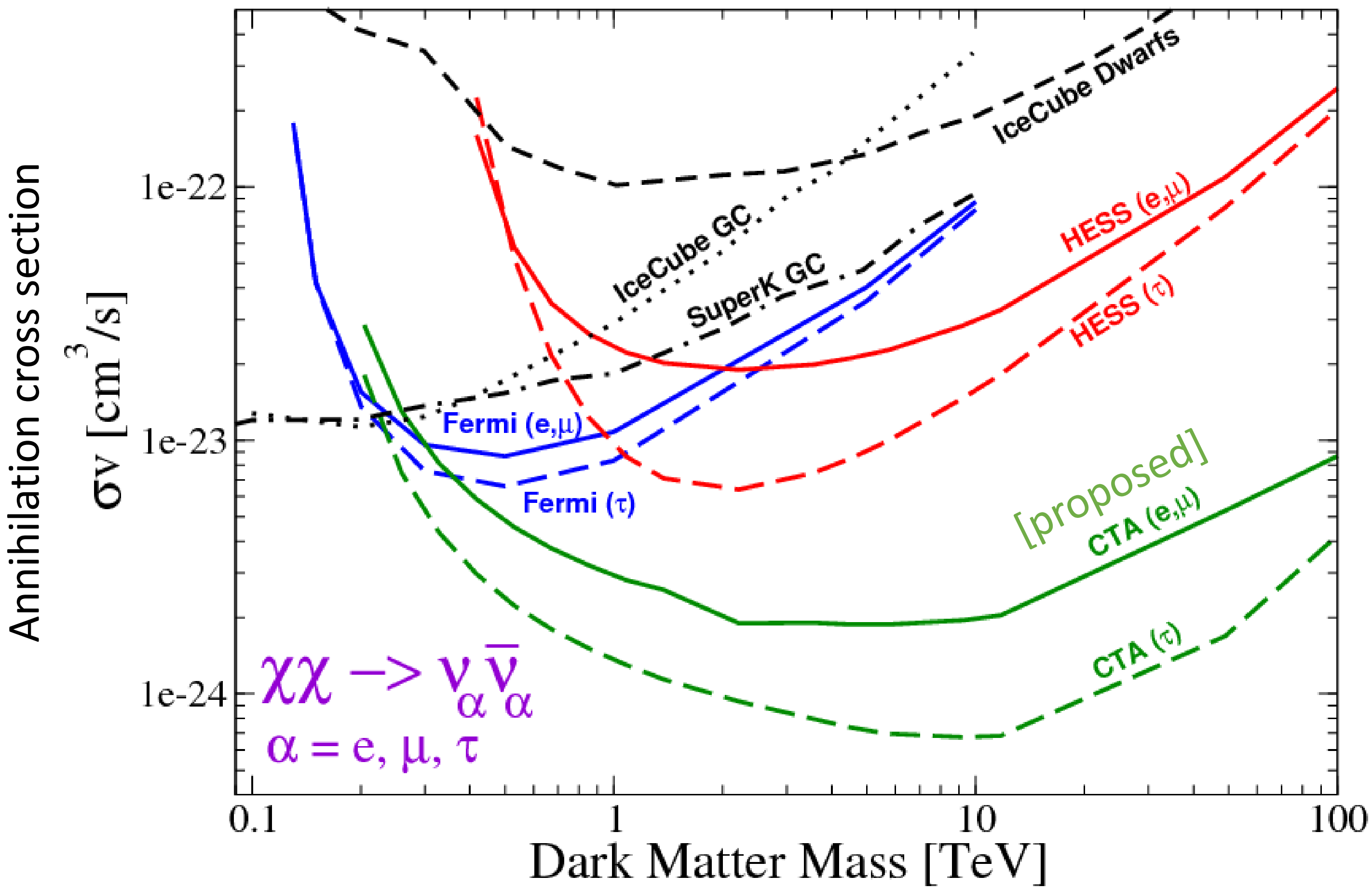

Su & Finkbeiner, arXiv:1206.1616

130 GeV line at the Galactic center?

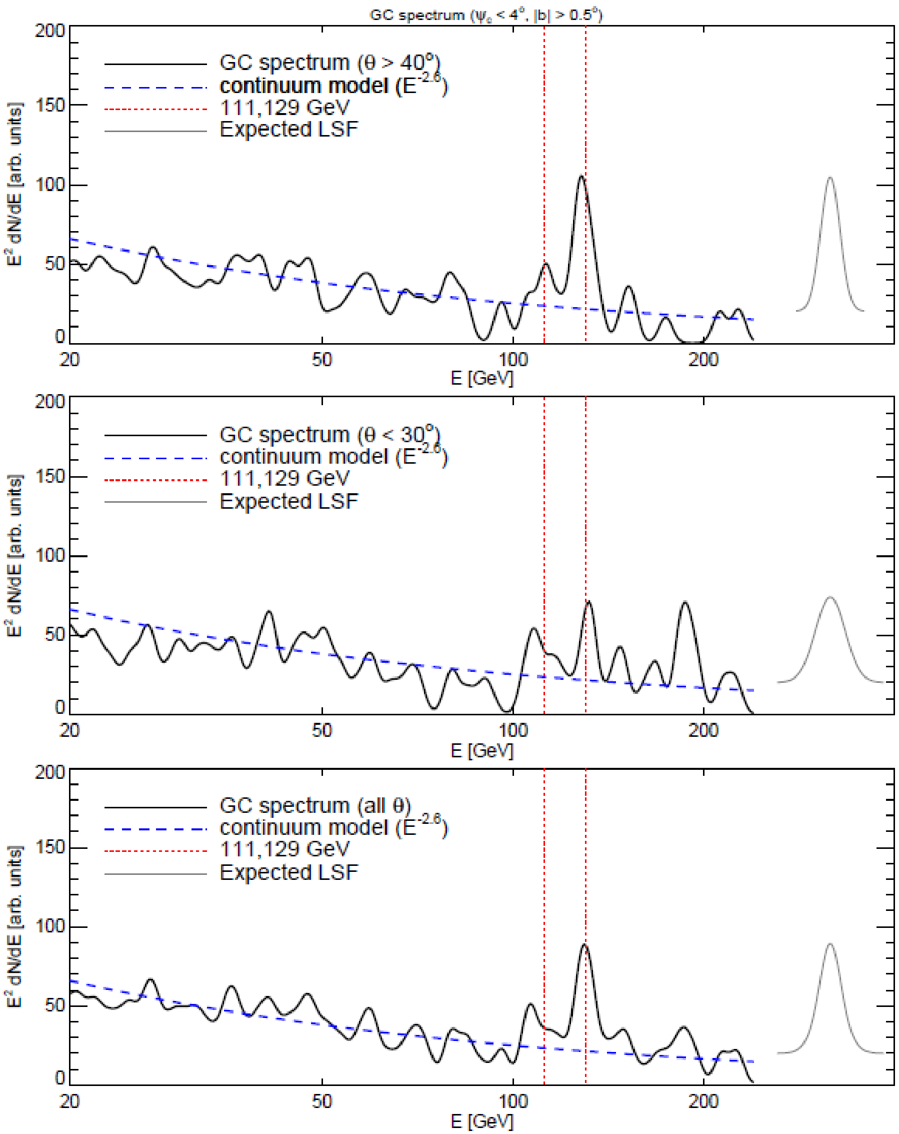

FIG. 18.— Spectrum of emission within 4° of the cusp center $(\ell, b) = (-1.5, 0)$, excluding $|b| < 0.5°$. High-incidence angle events (*upper panel*) have a factor of ~ 2 better energy resolution than those that enter the LAT close to normal incidence (*middle panel*) or the whole sample (*lower panel*). All three spectra have been smoothed by a Gaussian of 0.06 FWHM in $\Delta E/E$, similar to the expected resolution of the upper panel. The continuum model is $dN/dE \sim E^{-2.6}$, normalized at $20 < E < 50$ GeV (*blue dashed*).

Su, Finkbeiner & Weniger, JCAP 01(2013)209

130 GeV line at the Galactic center?

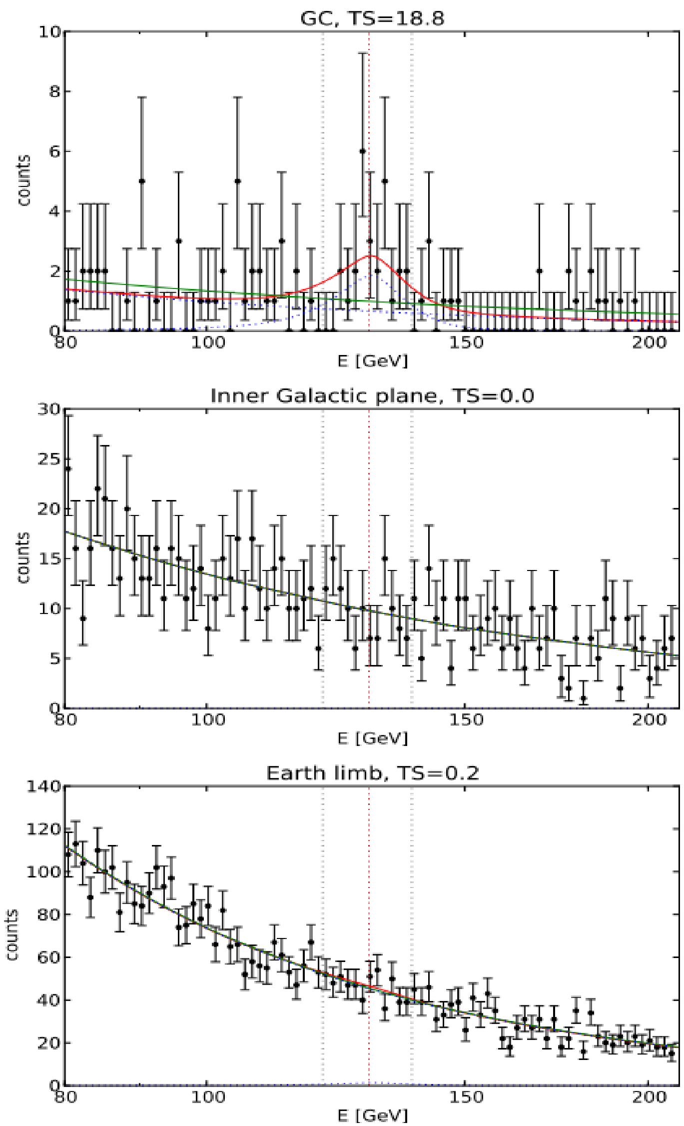

FIG. 3: Spectral fits to the GC, inner Galactic plane, and Earth limb samples. The green line shows the null model (a power-law), whereas the red line shows the alternative power-law + line fit; the dotted blue lines are the two components of the alternative model. The red (black) dotted lines indicate 129 GeV (13.6% FWHM around 129 GeV). Note that the significance found in the GC region does not represent the full significance of the putative signal.

TS=18.8 ↔ 4σ

Fermi-LAT dark matter line analysis (update)

M. ACKERMANN *et al.* PHYSICAL REVIEW D 91, 122002 (2015)

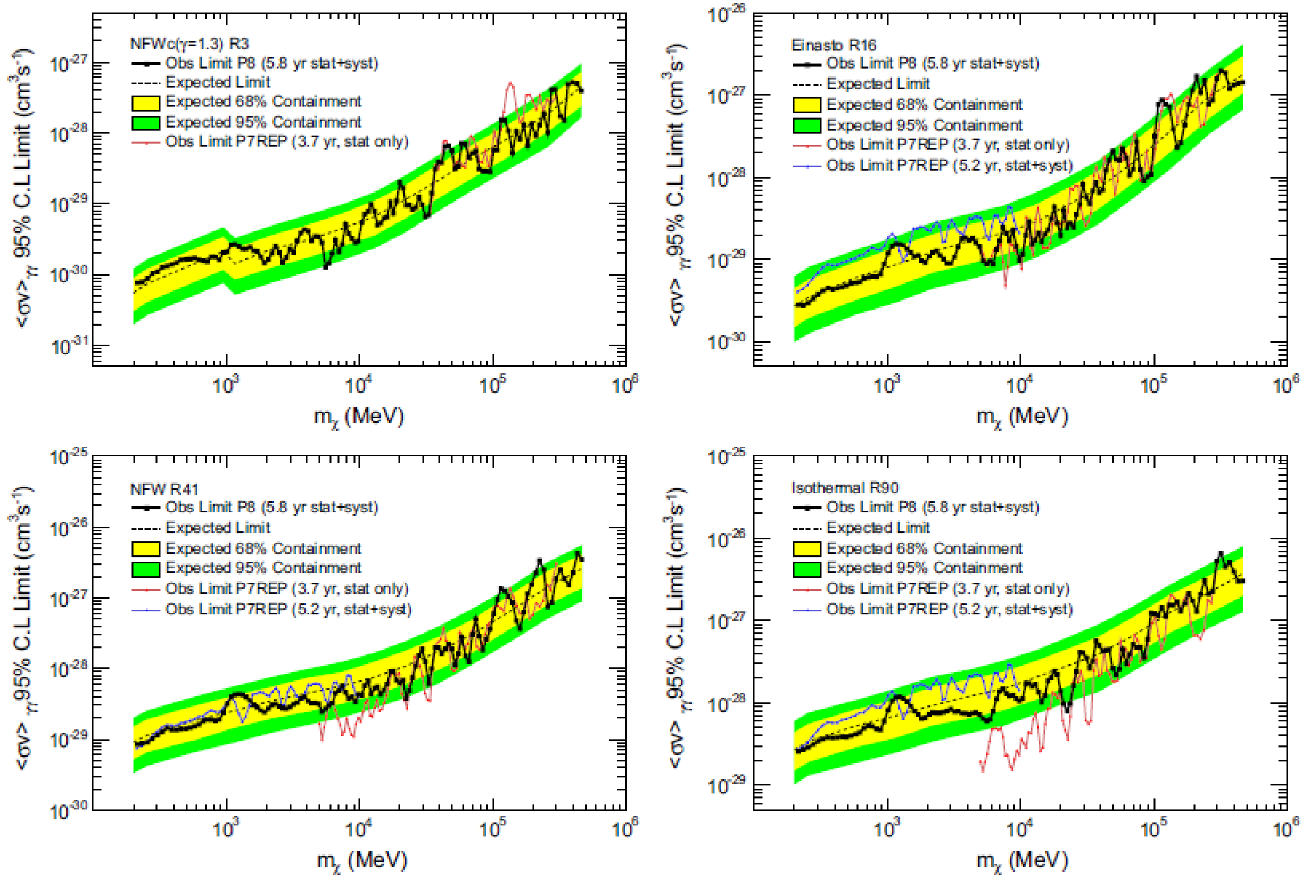

FIG. 8 (color online). 95% C.L. $\langle \sigma v \rangle_{\gamma\gamma}$ upper limits for each DM profile considered in the corresponding optimized ROI. The upper left panel is for the NFWc ($\gamma = 1.3$) DM profile in the R3 ROI. The discontinuity in the expected and observed limit in this ROI around 1 GeV is the result of using only PSF3-type events. See Sec. III for more information. The upper right panel is for the Einasto profile in the R16 ROI. The lower left panel is the NFW DM profile in the R41 ROI, and finally the lower right panel is the isothermal DM profile in the R90 ROI. Yellow (green) bands show the 68% (95%) expected containments derived from 1000 no-DM MC simulations (see Sec. V B). The black dashed lines show the median expected limits from those simulations. Also shown are the limits obtained in our 3.7-year line search [19] and our 5.2-year line search [22] when the assumed DM profiles were the same.

CALET gamma-ray spectrum

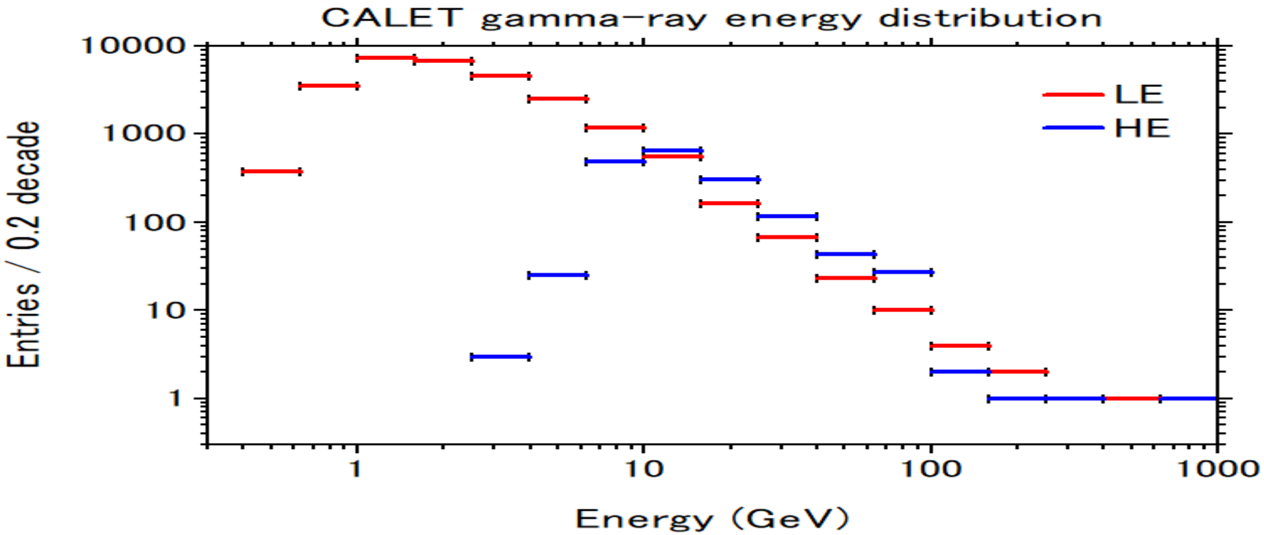

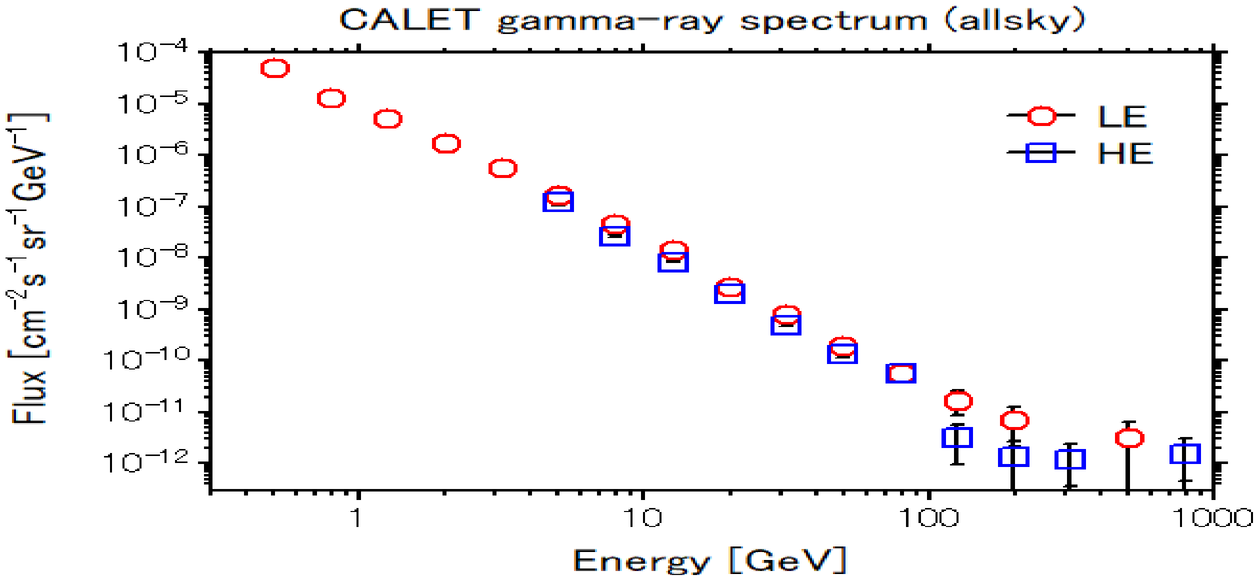

Effective area

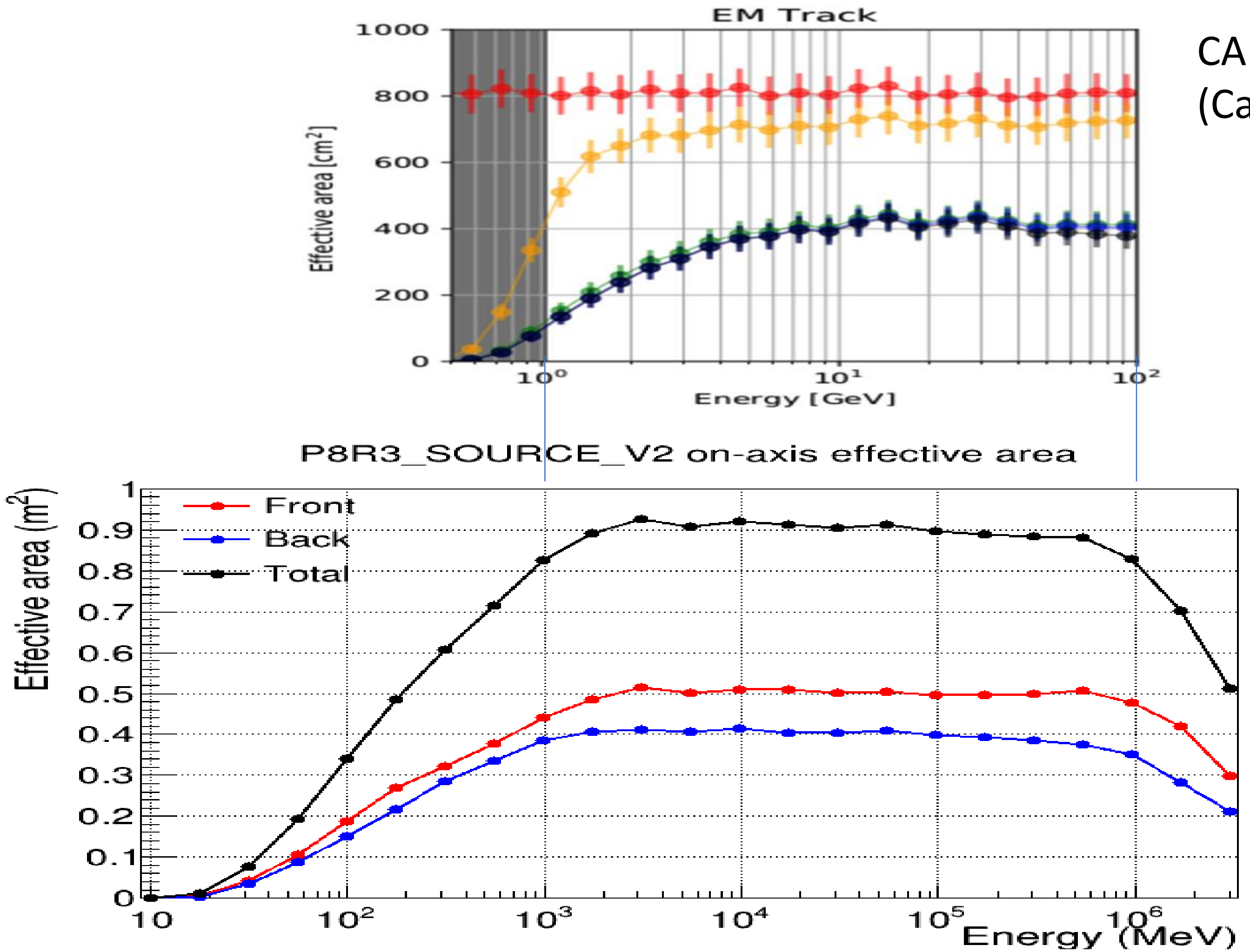

CALET LE γ
(Cannady+, 2018)

Fermi LAT

https://www.slac.stanford.edu/exp/glast/groups/canda/lat_Performance.htm

Energy resolution

CALET electron
(Asaoka+ 2017)

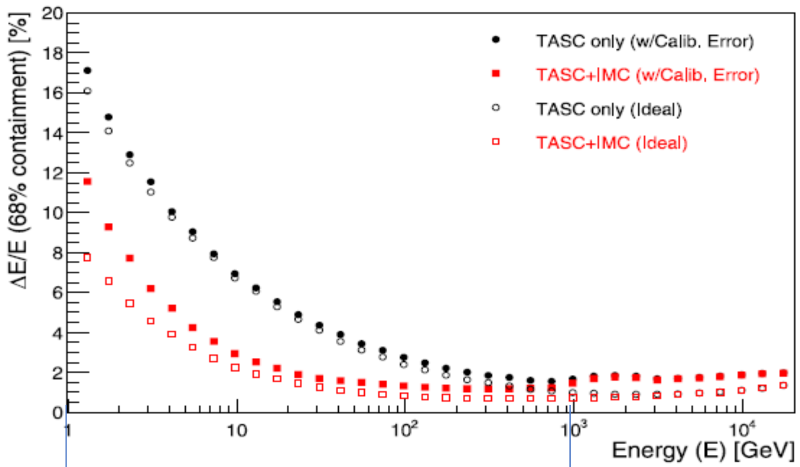

←2.5%@100 GeV

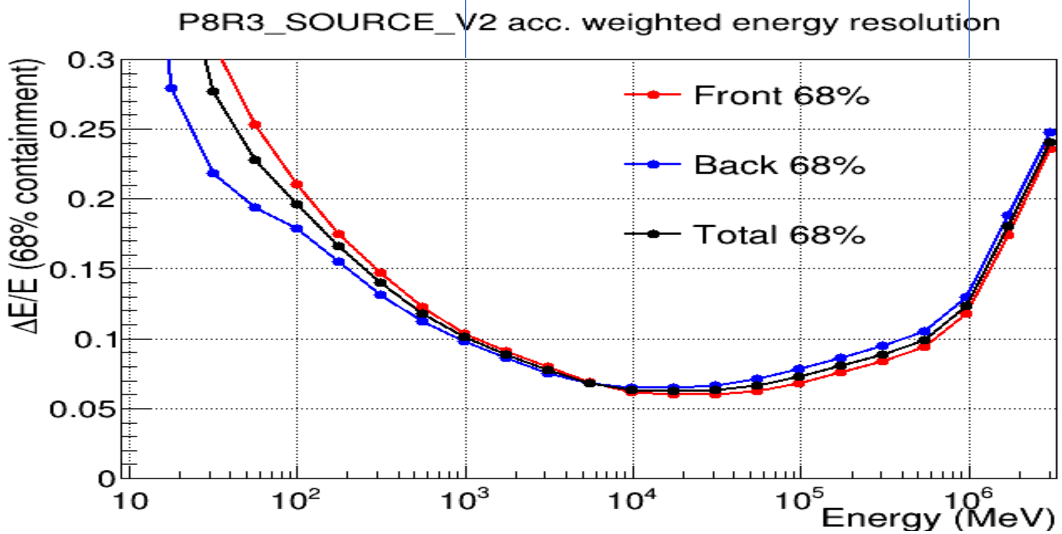

Fermi LAT

https://www.slac.stanford.edu/exp/glast/groups/canda/lat_Performance.htm

←7.5%@100 GeV

Angular resolution

100 GeV

C$_{68}$ [deg]

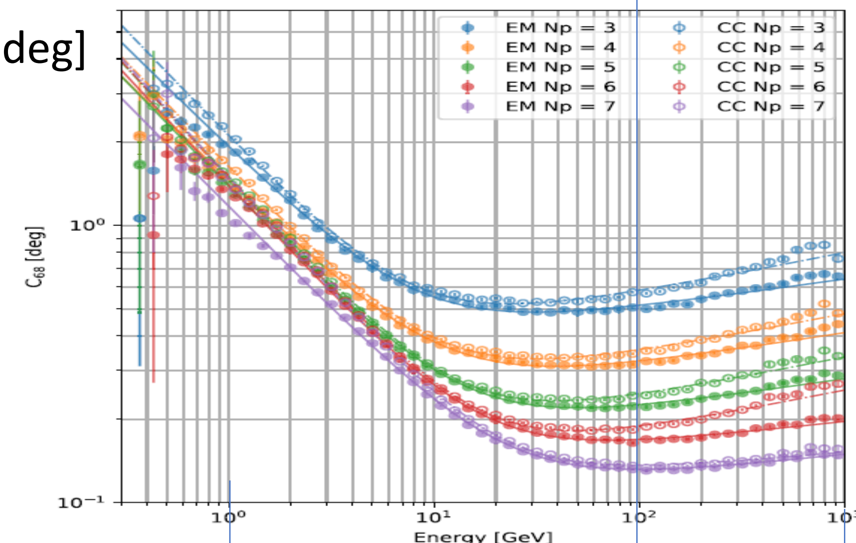

CALET LE γ
(Cannady+, 2018)

←0.6°@100 GeV

←0.13°@100 GeV

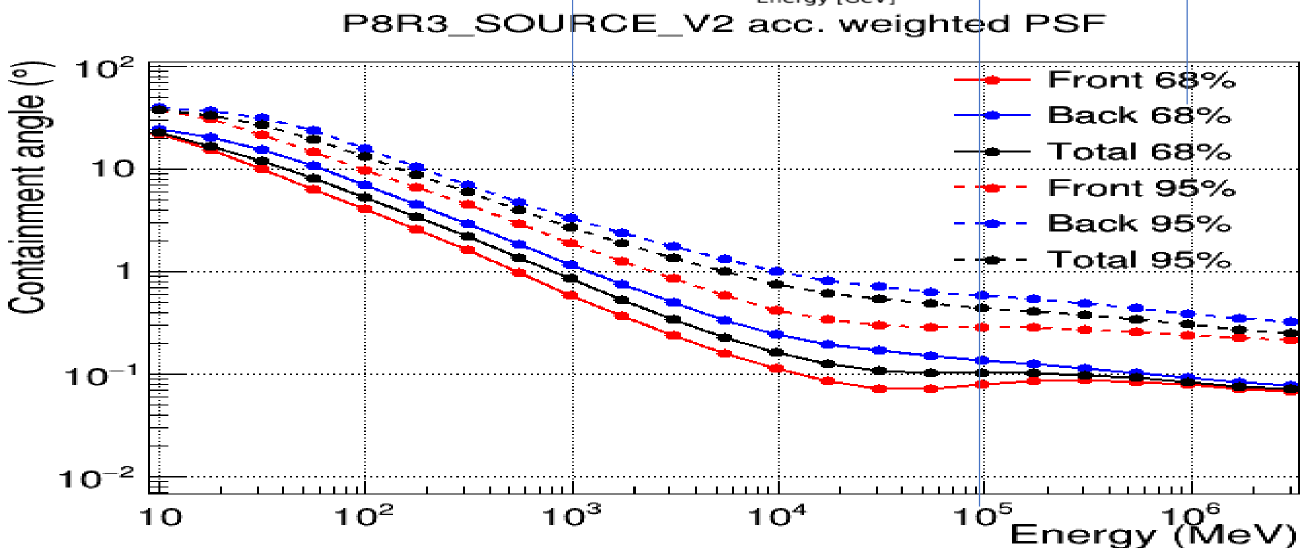

Fermi LAT

https://www.slac.stanford.edu/exp/glast/groups/canda/lat_Performance.htm

←0.1°@100 GeV

Point spread function: CALET vs LAT

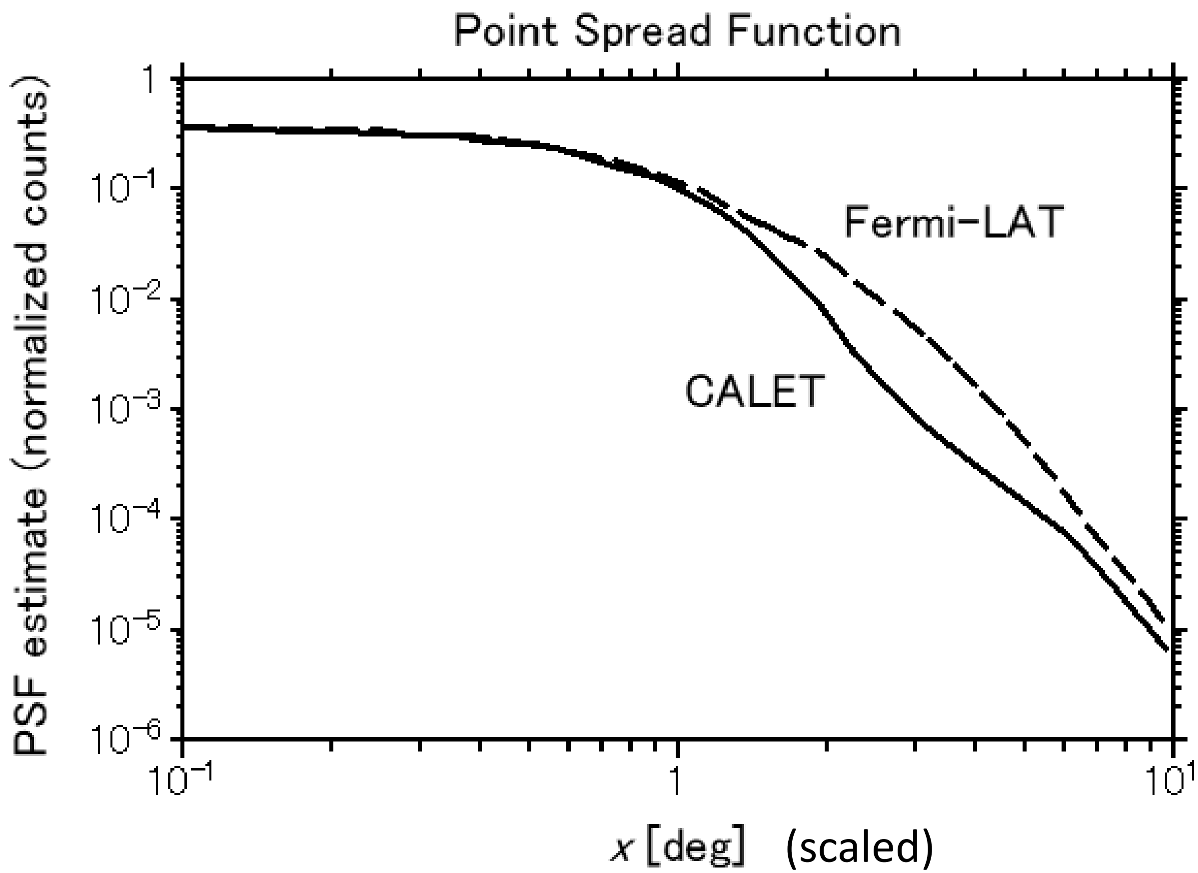

(scaled)

Effective area at high energies

Gamma ray, LE trig

100 GeV

Cannady+, 2018

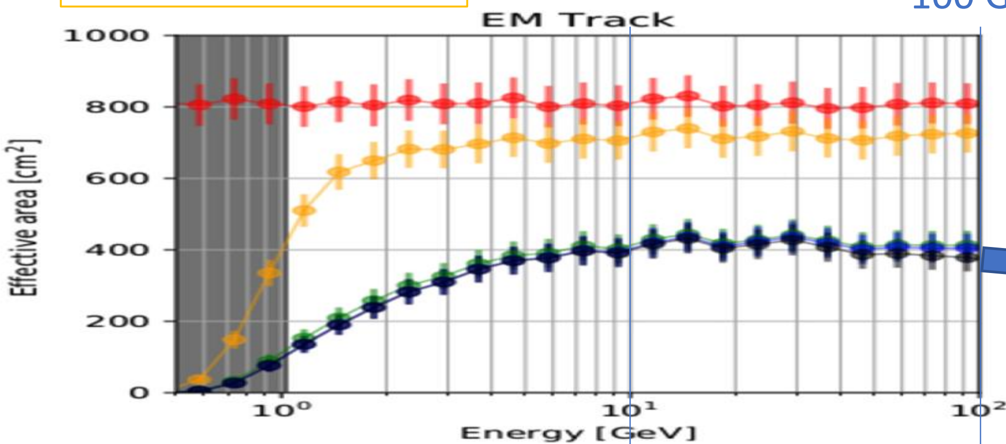

Decreasing…

→ *How to recover?*

Electron, HE trig

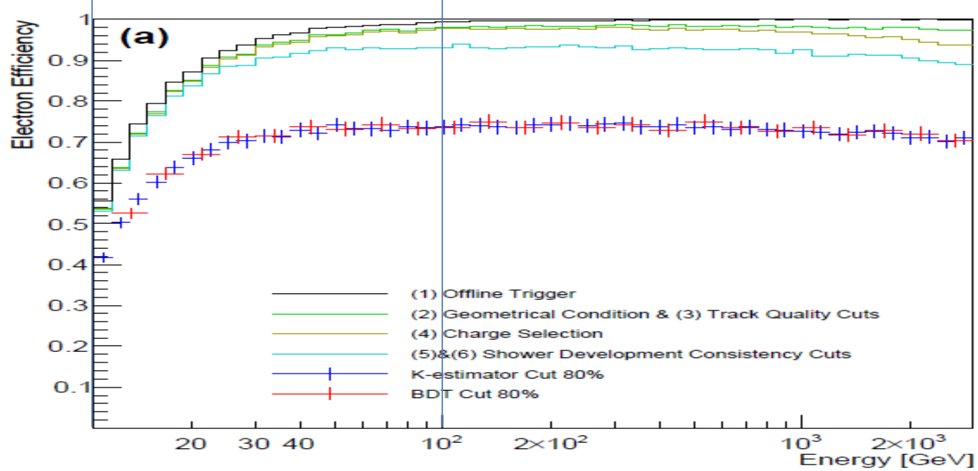

Adriani+, 2019

Efficiency in each step

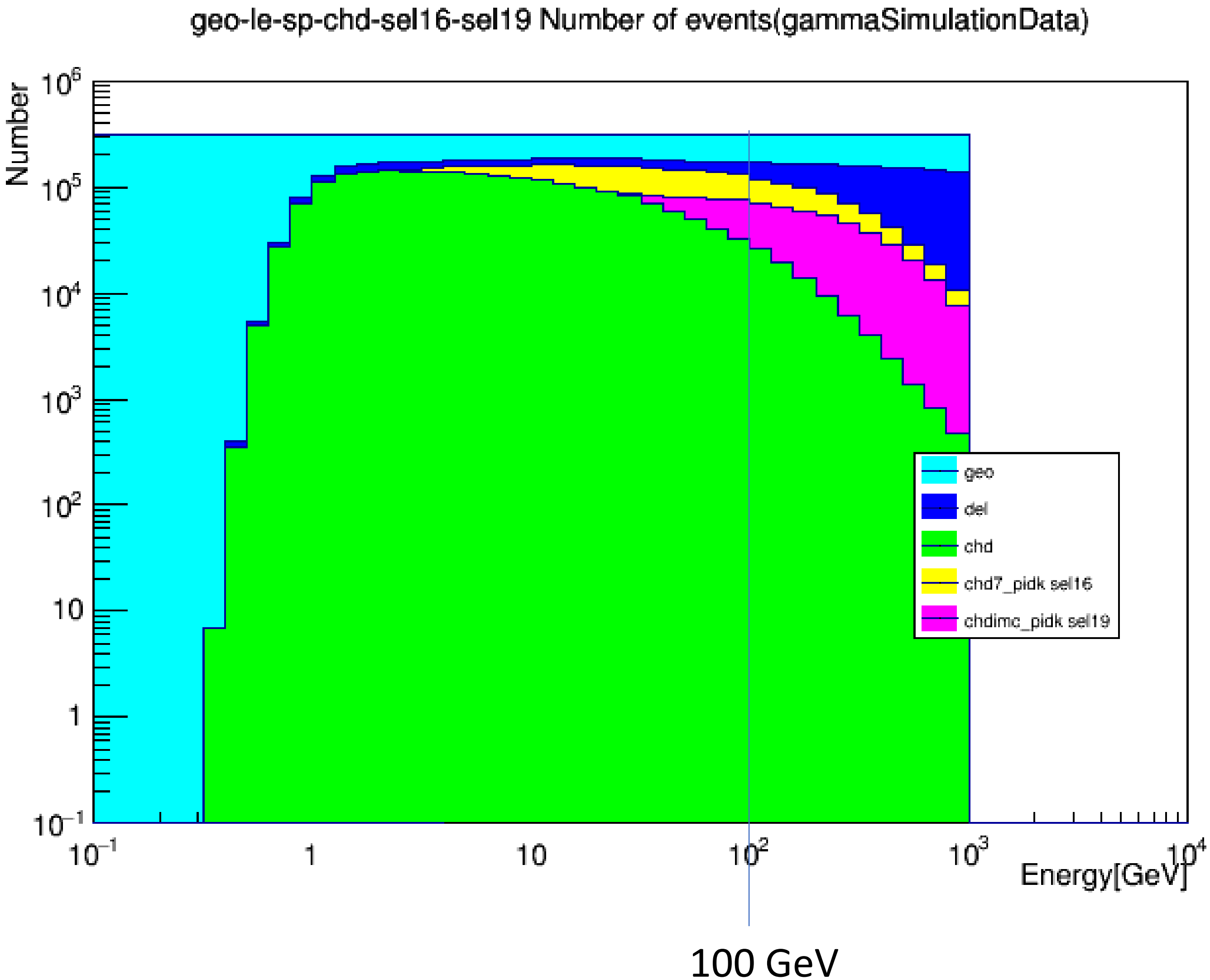

GW counterpart search

LIGO-VIRGO observation 3

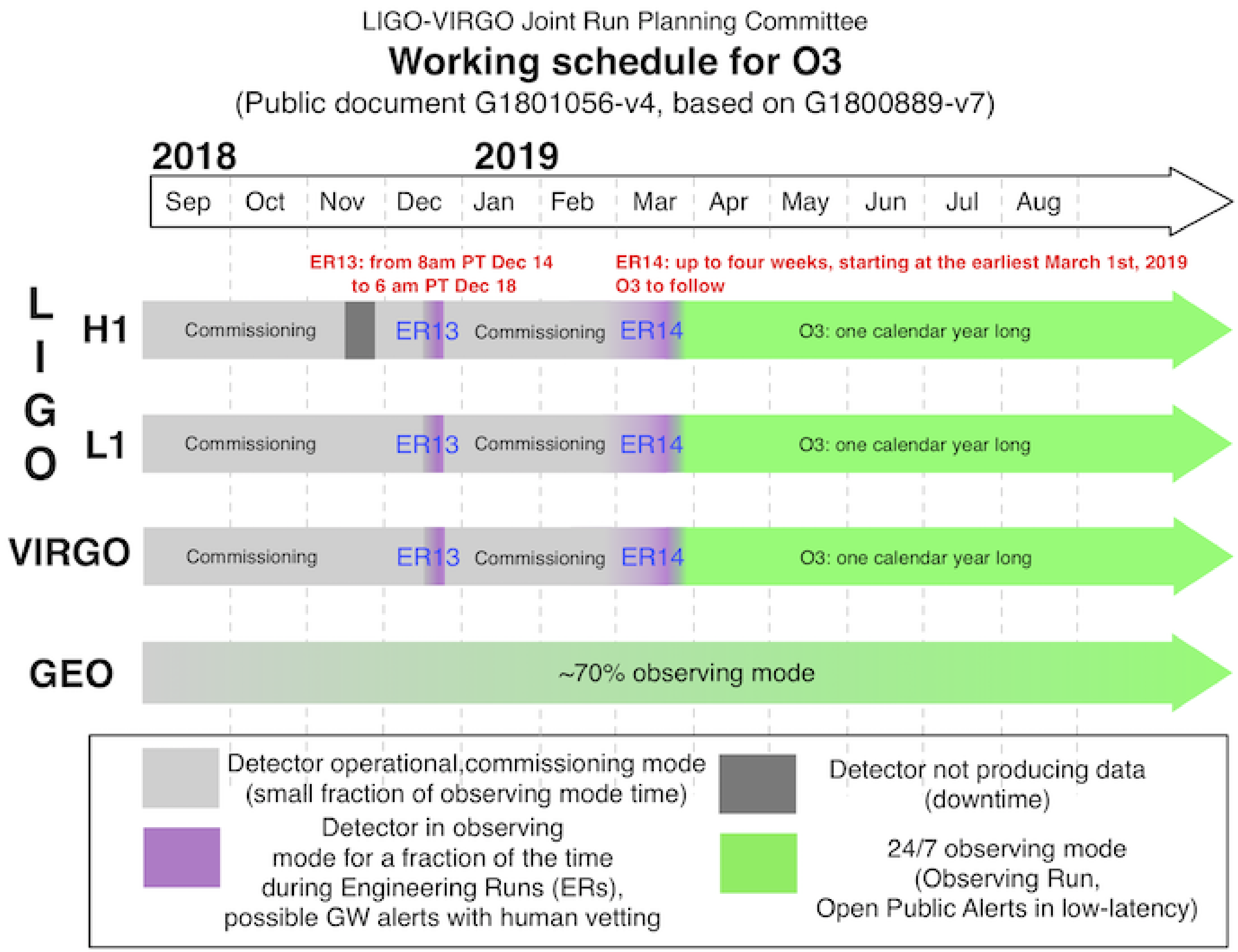

April 30, 2020

Mori, Asaoka et al., ICRC2019

Energy flux limit map for S190408an

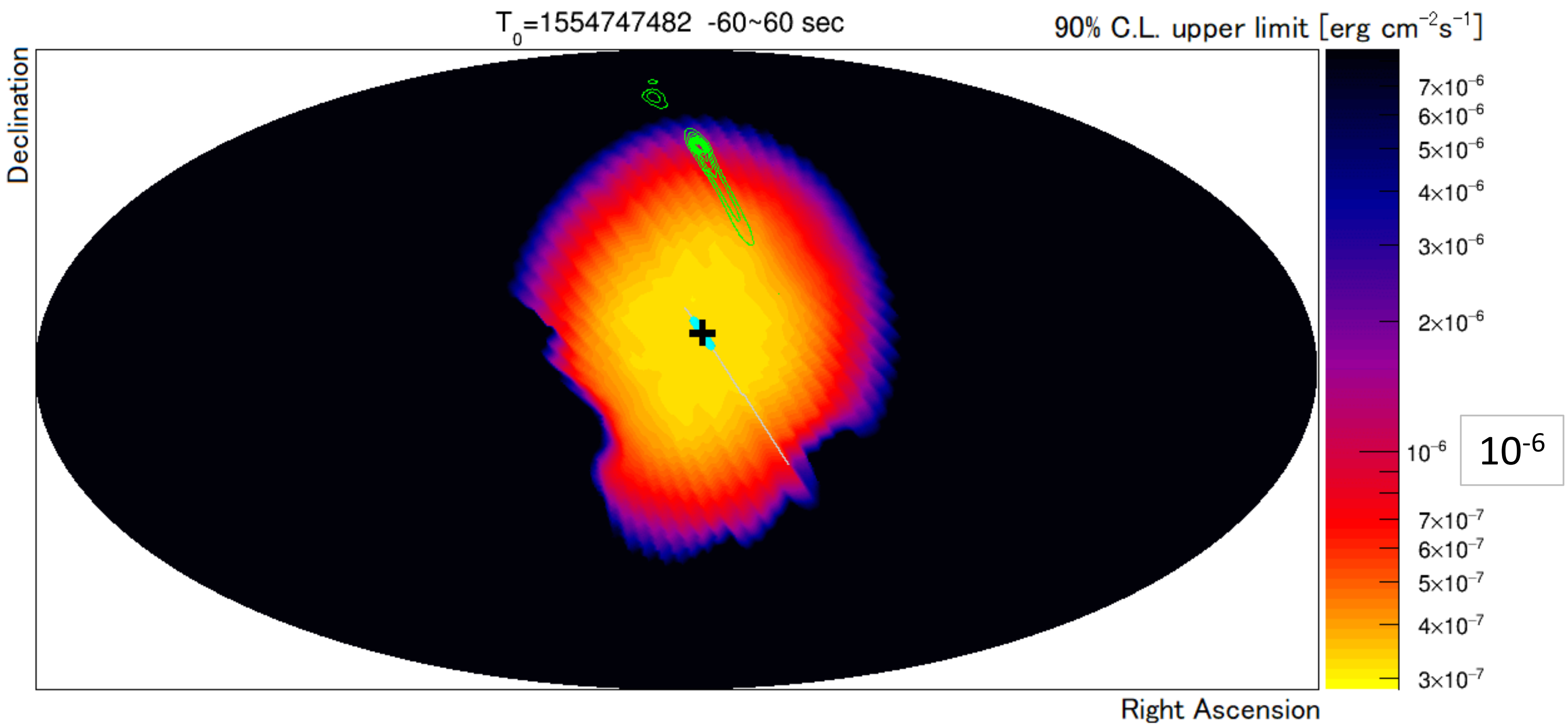

90% C.L. upper limit on S190408an energy flux in the energy region 1–10 GeV and time window [T_0-60s, T_0+60 s] shown in the equatorial coordinates. The thick cyan line shows the locus of the FOV center of CAL, and the plus symbol is that at T_0. Also shown by green contours is the localization significance map of S190408an reported by LIGO/Virgo.

Mori, Asaoka et al., ICRC2019

CAL limits on electromagnetic emission from gravitational wave events (LIGO/Virgo O3)

GCN No.	LIGO/Virgo trigger	Trigger time T_0 (2019)	Events $T_0 \pm 60$ s	90% C.L. U.L.	Summed probability	CAL α (°)	CAL δ (°)	Comments New!
24088	S190408an	04-08 18:18:02.288 UTC	0	2.3×10^{-6}†	80%	352.9	8.3	BBH (>99%)
24218	S190425z	04-25 08:18:05.017 UTC	0	1.0×10^{-4}	5%	131.3	-43.6	BNS (>99%)
24276	S190426c	04-26 15:21:55.337 UTC	0	2.5×10^{-5}	10%	183	-50.9	BNS (49%)
24403	S190503bf	05-03 18:54:04.294 UTC	0	4.2×10^{-5}	10%	169	-45.5	BBH (96%)
24495	S190510g	05-10 02:59:39.292 UT	0	–	No	295.7	50.8	Terrestrial (58%)
24531	S190512at	05-12 18:07:14.422 UT	0	1.9×10^{-5}	10%	214.9	37.7	BBH (99%)
24548	S190513bm	05-13 20:54:28.747 UT	0	6.0×10^{-5}†	5%	348	4.4	BBH (94%)
24593	S190517h	05-17 05:51:01.831 UT	0	–	No	126.2	-31.9	BBH (98%)
24617	S190519bj	05-19 15:35:44.398 UT	0	–	No	243.1	51.1	BBH (96%)
24648	S190521g	05-21 03:02:29.447 UT	0	6.0×10^{-6}	30%	205.7	49.2	BBH (97%)
24649	S190521r	05-21 07:43:59.463 UT	0	–	No	225.3	51.4	BBH (>99%)
24735	S190602aq	06-02 17:59:27.089 UT	0	2.9×10^{-4}	5%	127.5	45.1	BBH (99%)

Table 1: Summary of CALET/CAL gamma-ray observations on gravitational event candidates in the LIGO/Virgo third observing run reported in GCN circulars [1]. Upper limits (U.L.) are given in unit of erg cm^{-2}s^{-1} for the energy range 10–100 GeV except for those marked with † which are for 1–10 GeV, which corresponds to the HE and the LE-γ mode of the trigger condition of CAL around T_0. 'Summed probability' is the maximum probability in the overlap region of the CAL field-of-view at T_0 with the summed LIGO/Virgo probability map ('No' means there is no overlap). Also shown are the coordinates of the center of CAL field-of-view at T_0.

†: LE-γ

GraceDB glossary

- **BBH** - Binary black hole
- **BNS** - Binary neutron star
- **NSBH** - Neutron star black hole, a binary system composed of one neutron star and one black hole
- **Terrestrial** - Classification for signals in gravitational-wave detectors that are of instrumental or environmental origin. Terrestrial signals are not astrophysical and not due to gravitational waves. Some examples of sources of terrestrial signals are statistical noise fluctuations, detector glitches, and ground motion.
- **MassGap** - Compact binary systems with at least one compact object whose mass is in the hypothetical "mass gap" between neutron stars and black holes, defined here as 3-5 solar masses

Grace DB: https://gracedb.ligo.org/superevents/public/O3/

Extended to 12-SEP-2019

CAL limits on electromagnetic emission from gravitational wave events (LIGO/Virgo O3)

GCN No.	LIGO/Virgo trigger	Trigger time T_0 (2019)	Events $T_0 \pm 60$ s	90% C.L. U.L.	Summed probability	CAL α (°)	CAL δ (°)	Comments
24960	S190630ag	06-30 18:52:05.180 UT	0	1.2×10^{-5}	25%	84.0	31.5	BBH (94%)
24970	S190701ah	07-01 20:33:06.578 UT	0	–†	No	286.8	−1.6	BBH (93%)
25027	S190706ai	07-06 22:26:41.345 UT	0	–	No	210.4	−45.4	BBH (99%)
25033	S190707q	07-07 09:33:26.181 UT	0	2.1×10^{-6}†	20%	262.4	2.2	BBH (>99%)
25099	S190718y	07-18 14:35:12.068 UT	0	1.7×10^{-6}†	5%	195.8	−11.1	Terrestrial (98%)
25134	S190720a	07-20 00:08:36.704 UT	0	3.0×10^{-5}	25%	49.7	−32.1	BBH (99%)
25184	S190727h	07-27 06:03:33.986 UT	0	–	No	201.1	38.2	BBH (92%)
25214	S190728q	07-28 06:45:10.529 UT	0	–†	No	184.8	30.3	BBH (95%)
25390	S190814bv	08-14 21:10:39.013 UT	0	–	No	181.3	49.5	NSBH (>99%)
25536	S190828j	08-28 06:34:05.756 UT	0	–	No	13.9	12.6	BBH (>99%)
25537	S190828l	08-28 06:55:09.887 UT	0	–	No	106.9	51.0	BBH (>99%)
25647	S190901ap	09-01 23:31:01.838 UT	0	6.3×10^{-5}†	5%	353.8	16.6	BNS (86%)

Table 1: Summary of CALET/CAL gamma-ray observations on gravitational event candidates in the LIGO/Virgo third observing run reported in GCN circulars [1]. Upper limits (U.L.) are given in unit of erg cm^{-2}s^{-1} for the energy range 10–100 GeV except for those marked with † which are for 1–10 GeV, which corresponds to the HE and the LE-γ mode of the trigger condition of CAL around T_0. 'Summed probability' is the maximum probability in the overlap region of the CAL field-of-view at T_0 with the summed LIGO/Virgo probability map ('No' means there is no overlap). Also shown are the coordinates of the center of CAL field-of-view at T_0.

†: LE-γ

Extended further to 27-JAN-2020

CAL limits on electromagnetic emission from gravitational wave events

(LIGO/Virgo O3)

GCN No.	LIGO/Virgo trigger	Trigger time T_0 (2019)	Events $T_0 \pm 60$ s	90% C.L. U.L.	Summed probability	CAL α (°)	CAL δ (°)	Comments
25734	S190910d	09-10 01:26:19 UT	0	–†	No	100.8	22.9	NSBH (98%)
25735	S190910h	09-13 03:38:21 UT	0	9.4×10^{-6}†	10%	294.8	-5.5	BNS (61%)
25770	S190915ak	09-15 23:57:02 UT	0	–	No	99.7	-11.1	BBH (99%)
25830	S190923y	09-23 12:55:59 UT	0	1.2×10^{-5}	10%	55.3	-2.5	NSBH (68%)
25844	S190924h	09-24 02:18:46 UT	0	–	No	273.4	40.2	MassGap (>99%)
25891	S190930s	09-30 13:35:41 UT	0	3.5×10^{-5}	5%	20.7	-3.3	MassGap (95%)
25892	S190930t	09-30 14:34:07 UT	0	1.7×10^{-5}	5%	235.5	36.3	NSBH (74%)
26195	S191105e	11-05 14:35:21 UT	0	–	No	223.0	-27.4	BBH (95%)
26236	S191109d	11-09 01:07:17 UT	0	–	No	349.6	-16.6	BBH (>99%)
26237	S191110af	11-10 23:06:44 UT	0	8.4×10^{-6}	40%	218.6	-42.7	–
26321	S191129u	11-29 13:40:29 UT	0	–	No	356.9	50.7	BBH (>99%)
26358	S191204r	12-04 17:15:26 UT	0	–	No	269.2	34.3	BBH (>99%)
26377	S191205ah	12-05 21:52:08 UT	0	–	No	80.2	-32.8	NSBH (93%)
26419	S191213g	12-13 04:34:08 UT	0	–	No	20.4	-9.3	BNS (77%)
26465	S191215w	12-15 22:30:52 UT	0	–	No	222.3	40.3	BBH (>99%)
26481	S191216ap	12-16 21:33:38 UT	0	–†	No	186.8	13.9	BBH (99%)
26602	S191222n	12-22 03:35:37 UT	0	–†	No	330.3	-2.1	BBH (>99%)
26664	S200105ae	01-05 16:24:26 UT	0	6.5×10^{-6}	60%	50.6	-30.6	NSBH (3%)
26740	S200112r	01-12 15:58:38 UT	0	1.1×10^{-6}	5%	84.7	40.0	BBH (>99%)
26761	S200114f	01-14 02:08:18 UT	0	4.7×10^{-6}	80%	111.2	50.7	–
26797	S200115j	01-15 04:23:09 UT	0	1.7×10^{-6}	20%	84.4	45.9	MassGap (>99%)

†: LE-γ

LIGO-VIRGO O3: Monthly variation

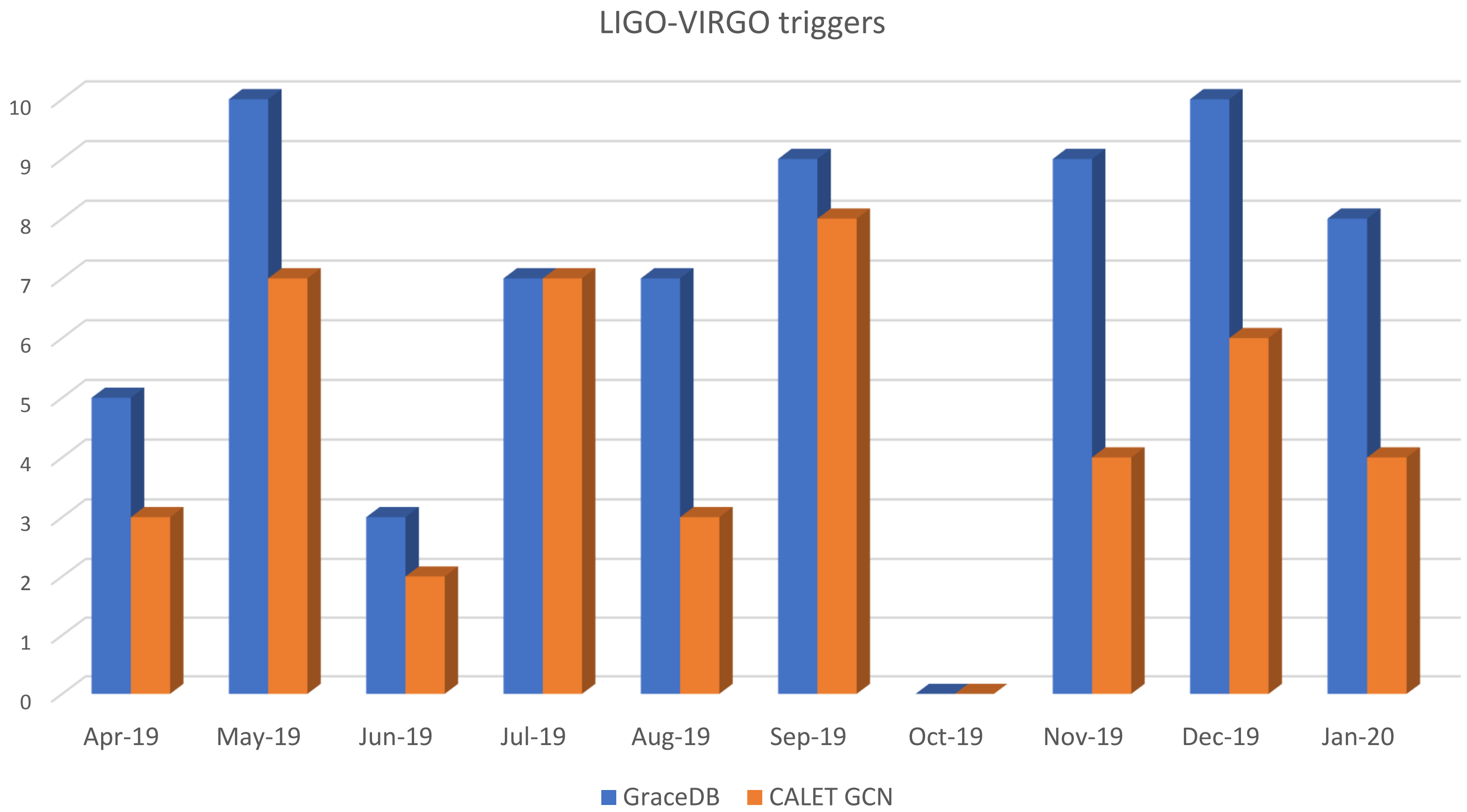

Grace DB: https://gracedb.ligo.org/superevents/public/O3/

Mori, ICRC2019

Searching transient events

- Gamma ray bursts, AGN flares, EM counterparts of GW, …
- We define a 'transient event' as a gamma-ray pair coming from the same direction (within our angular resolution) in a 120-s time window.

Judging 'pairs' using PSF

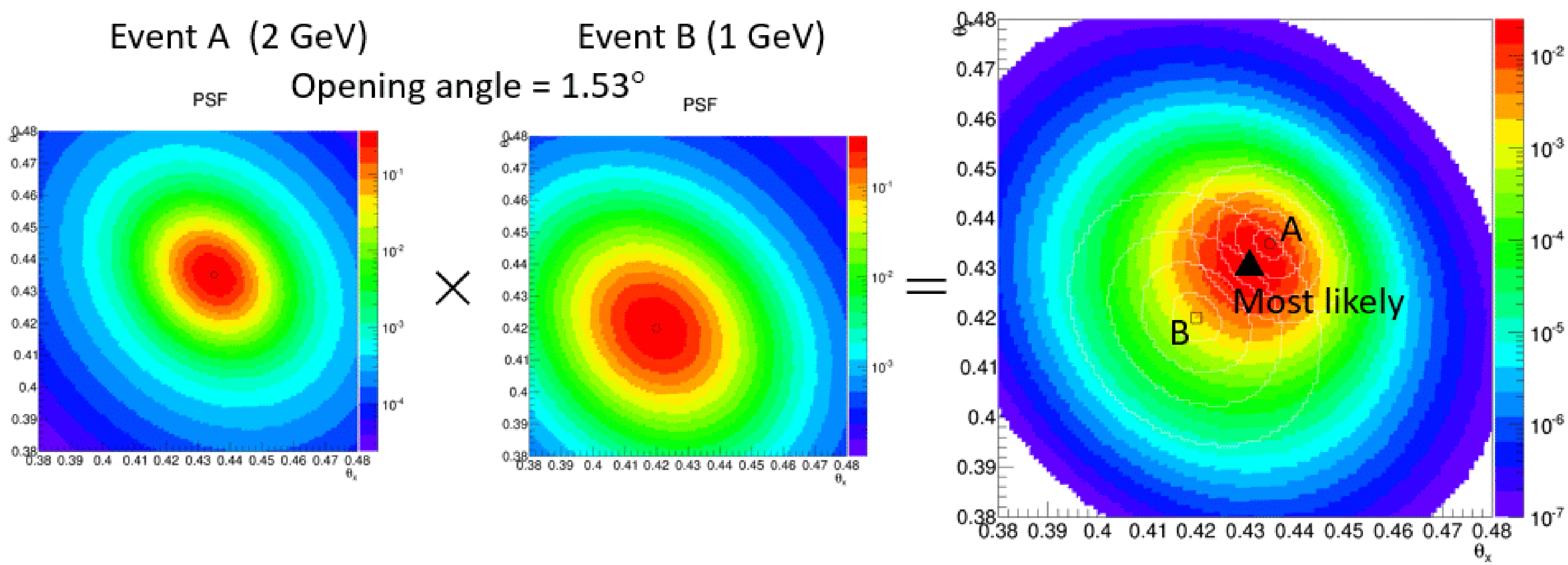

See also poster PS3-243 (Cannady et al.) for GRB search by CALET/CAL

Mori, ICRC2019

Transient gamma-ray monitor system

- Running since 2018/08/20 at WCOC
- Parallel processing (60 threads) – 40 min for 1hr data

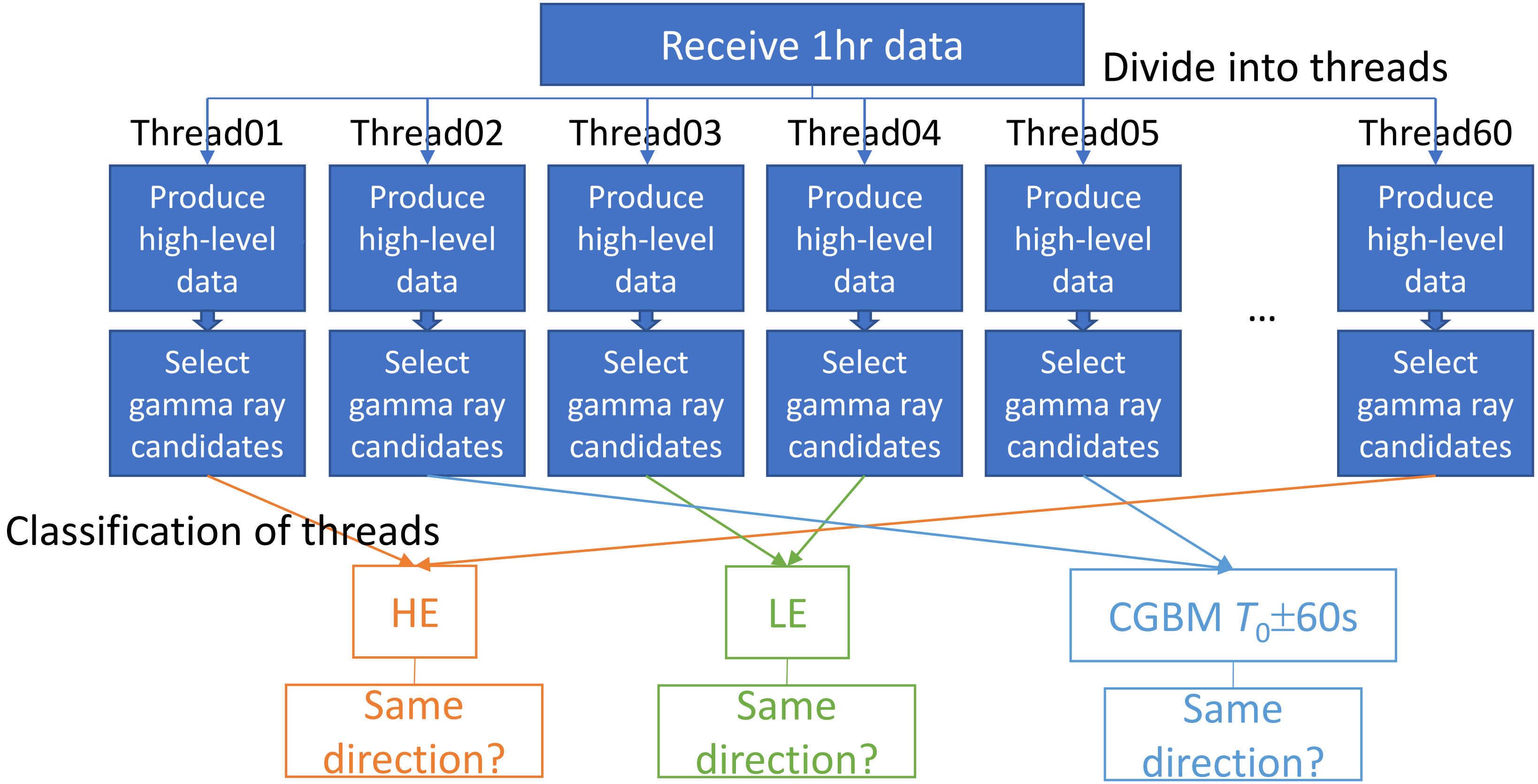

WCOC DQC “GAM_PAIRS”

CALET WCOC Web Tool QL DQC

fov_info 2	181220T20:25	TBD	JEMRMS Parked at Stowed

191229 GAM_PAIRS

Pair event list

try77

EventID_1	EventID_2	Probability	(R.A, Dec) [degree]	Opening angle [degree]	MDCTIME [s]	UT [s]	Time difference [s]	Energy_1 [GeV]	Energy_2 [GeV]	(dir0_1, dir1_1)	(dir0_2, dir1_2)
31522	43347	0.136	(128.800, -45.093)	0.444	1261636038	2019/12/29 06:30:07.045266	289.191015	1.298	4.277	(-0.251, 0.561)	(-0.497, 0.543)

No pairs were found with try17.

Event display

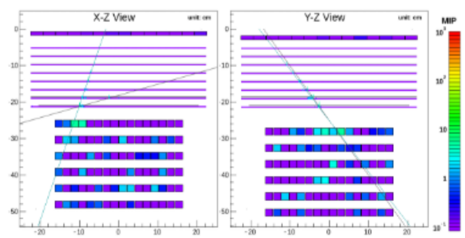

Event display for EventID: 31522

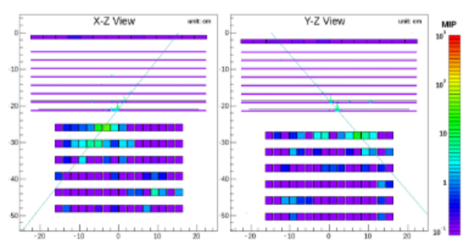

Event display for EventID: 43347

DAQ DSZ TMP TRG SPC GPS ASC L1C GAM GAM_PAIRS LEE FIL PED
Prev Prev Week HOME Next week Next
fov_info 2 | 181220T20:25 | TBD | JEMRMS Parked at Stowed

Summary

- Gamma ray analysis is on-going.
- We have to recover efficiencies toward higher energies to have enough statistics. Some new idea is necessary.
- Dark matter line signal search could be sensitive thanks to our good energy resolution.
- GW counterpart search results are regularly reported in GCN circulars, but we have only upper limits up to now.
- Automated search for gamma-ray pairs are working at WCOC.

Backups

Mori, Asaoka et al., ICRC2019

Gamma-ray spectra

LE-γ mode
from 2015 November to 2018 May

"On-plane": $|l|$ < 80° & $|b|$< 8°

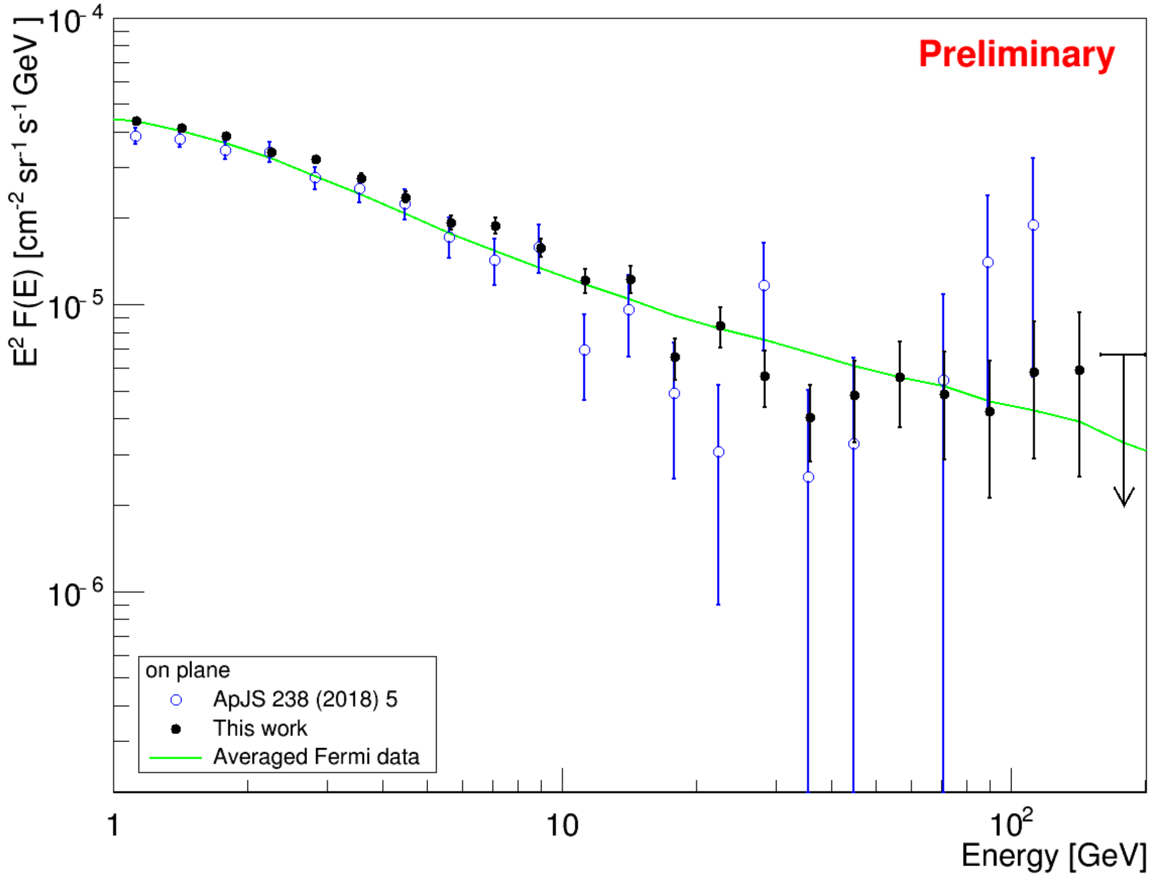

Monitoring count rates of AGNs

- Search for flares of known AGNs
- Use events within 68% containment angles from AGNs listed in 3FGL (Fermi-LAT 4-year catalog)
- Calculate count rates based on 28-day exposures assuming E^{-2} spectra

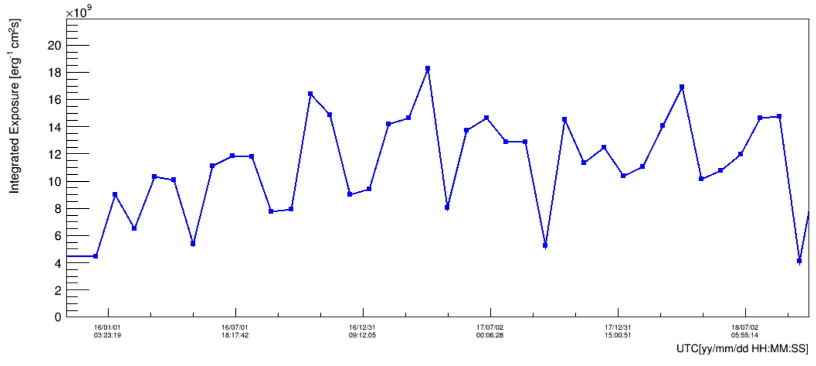

Exposures for CTA102 (2015/11-2018/09)

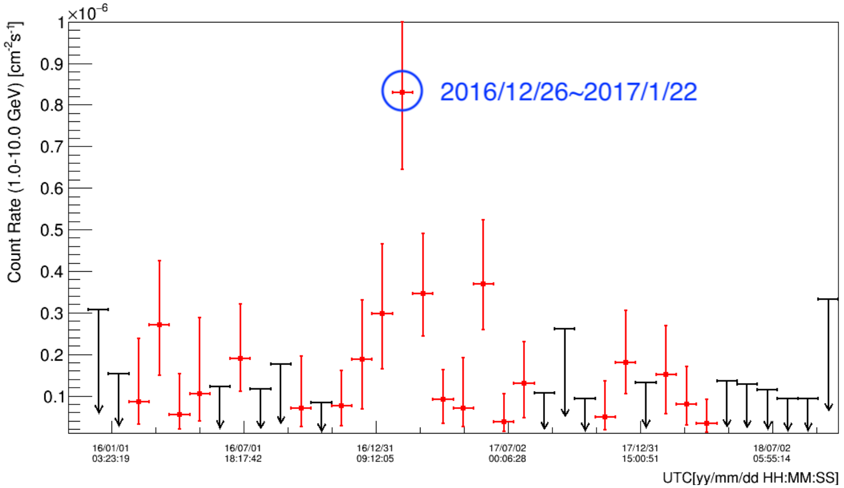

Count rates for CTA102 (2015/11-2018/09)

Monitoring count rates of AGNs

- Search for flares of known AGNs
- Use events within 68% containment angles from AGNs listed in 3FGL (Fermi-LAT 4-year catalog)
- Calculate count rates based on 28-day exposures assuming E^{-2} spectra

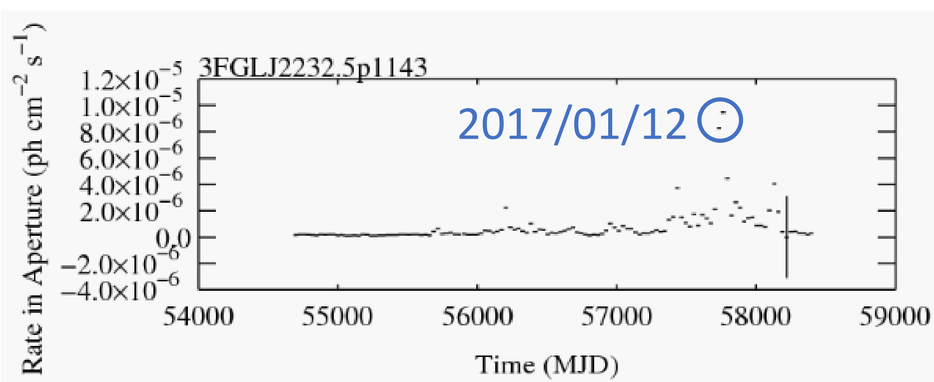

Fermi-LAT count rates for CTA102

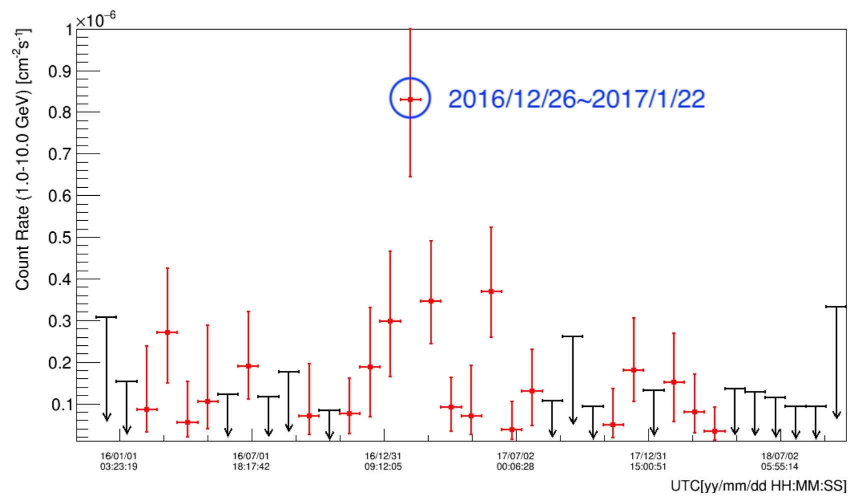

Count rates for CTA102 (2015/11-2018/09)

Summary for part B

- Selection algorithm for transient gamma-ray events has been developed with FOV cut and direction consistency. It could identify point sources.
- 503 CGBM triggers are analyzed ($T_0 \pm 60$s) but no pairs were found.
- Monitoring method for count rates of AGNs has been developed. It could identify CTA102 flare (2017/01).
- Transient gamma-ray monitor system is running since 2018/08. It can detect transient events within 2hr from CGBM triggers by parallel processing.

Analysis of TXS 0506+056/IceCube-170922A

- 2015/10/13-2018/05/31, LEγ run, FOV cut (fixed structure & robot arm)

EM track

CC track

Light curve
(1day/bin,
2months/tic)

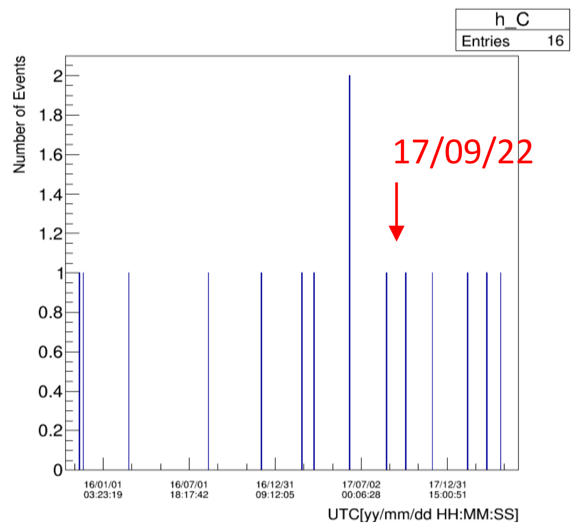

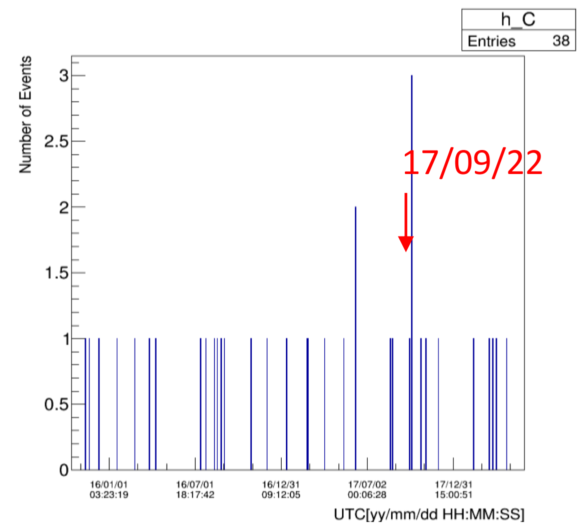

Countmap
(within 2°)

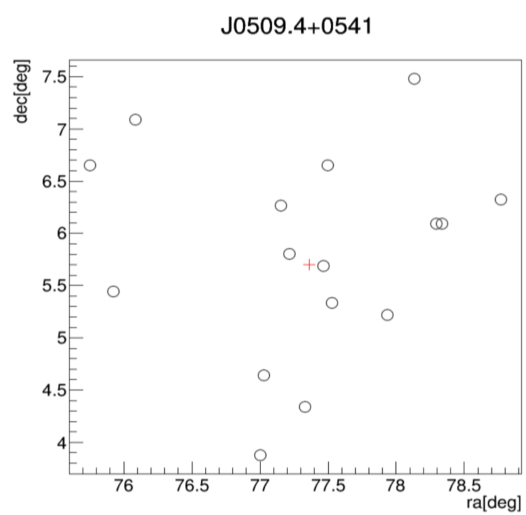

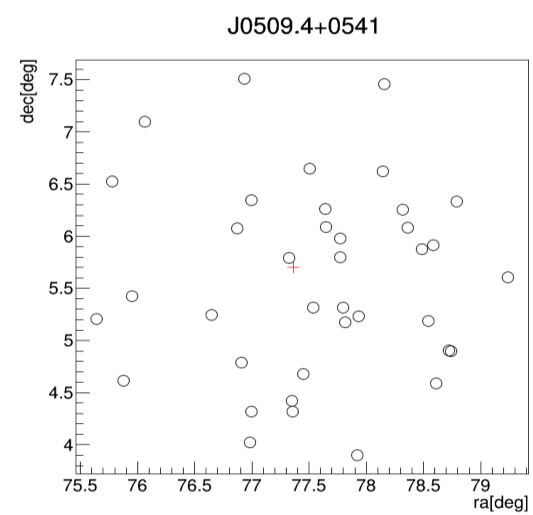

+ : TXS 0506+056

Analysis of TXS 0506+056/IceCube-170922A

EM track

CC track

Integrated Exposure

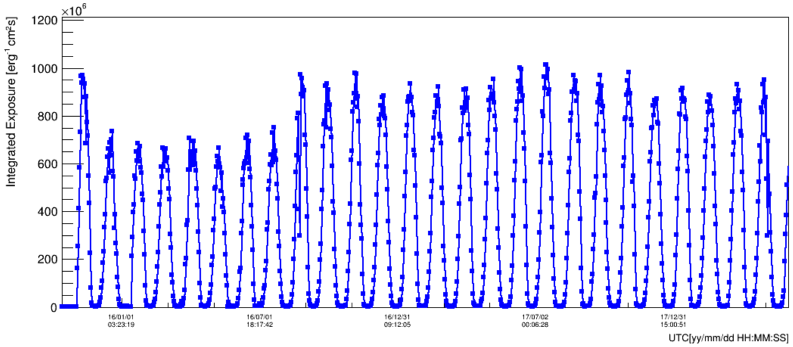

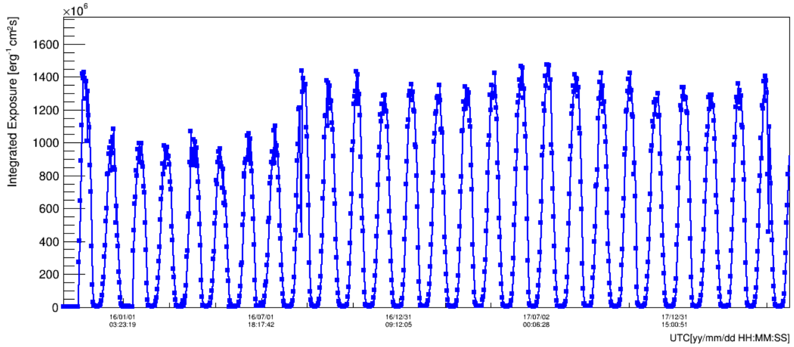

Integrated Flux

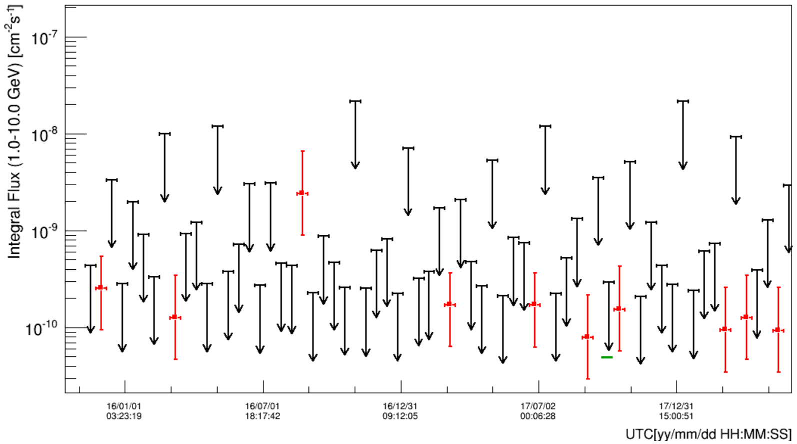

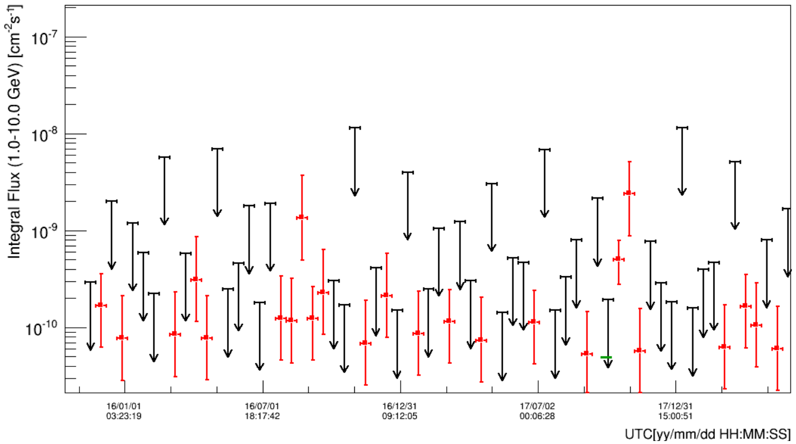

Analysis of TXS 0506+056/IceCube-170922A

EM track

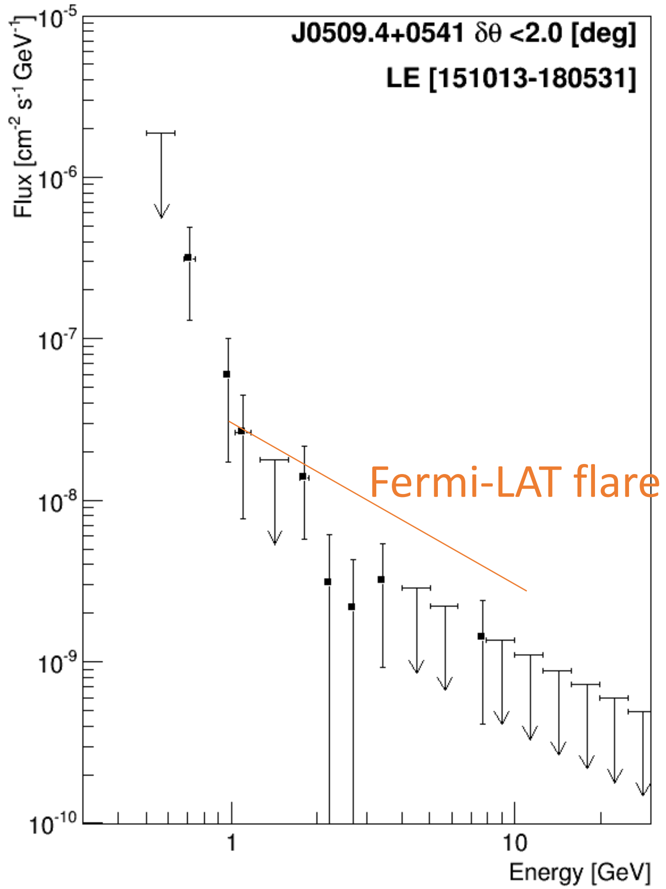

CC track

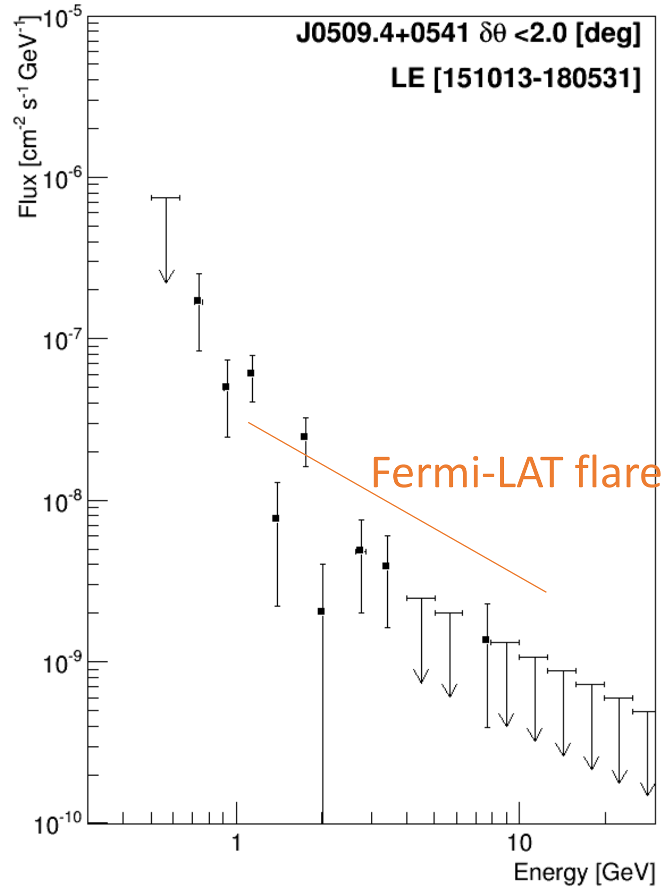

Cf. Fermi-LAT: 3.6×10^{-7}cm^{-2}s^{-1} (0.1-300 GeV, Sep.15-27 2017; Atel #10791)

$\rightarrow$ $dN/dE = 3.6 \times 10^{-8} (E/GeV)^{-2}$ cm^{-2}s^{-1}GeV^{-1}

Effective Area and Sensitivity

Effective area is estimated as a function of incident angle (dx/dz, dy/dz) and energy. Maximum effective area is achieved at around 5 GeV, but lower energy is more important for steep spectrum like E^{-2}.

LE-γ trigger: > 1 GeV
HE trigger: > 10 GeV

3-10GeV average

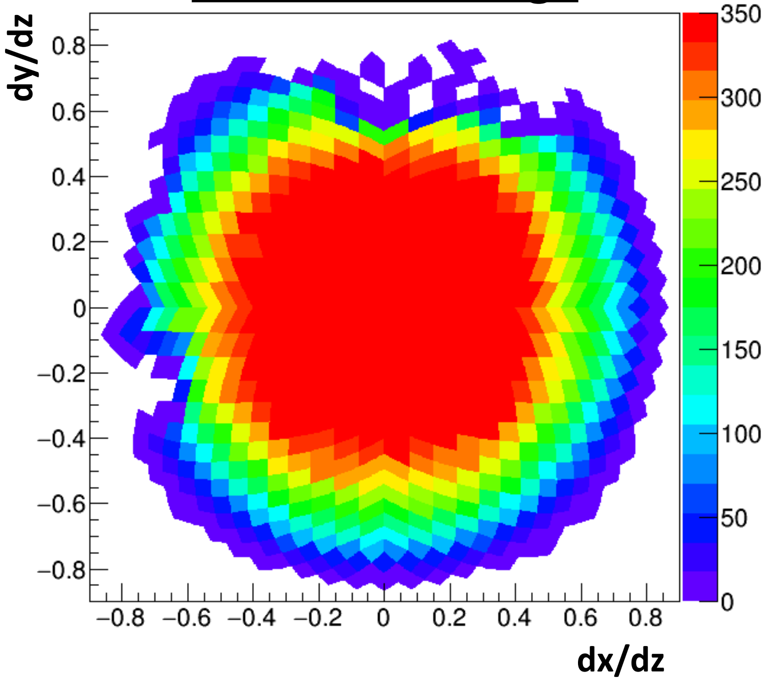

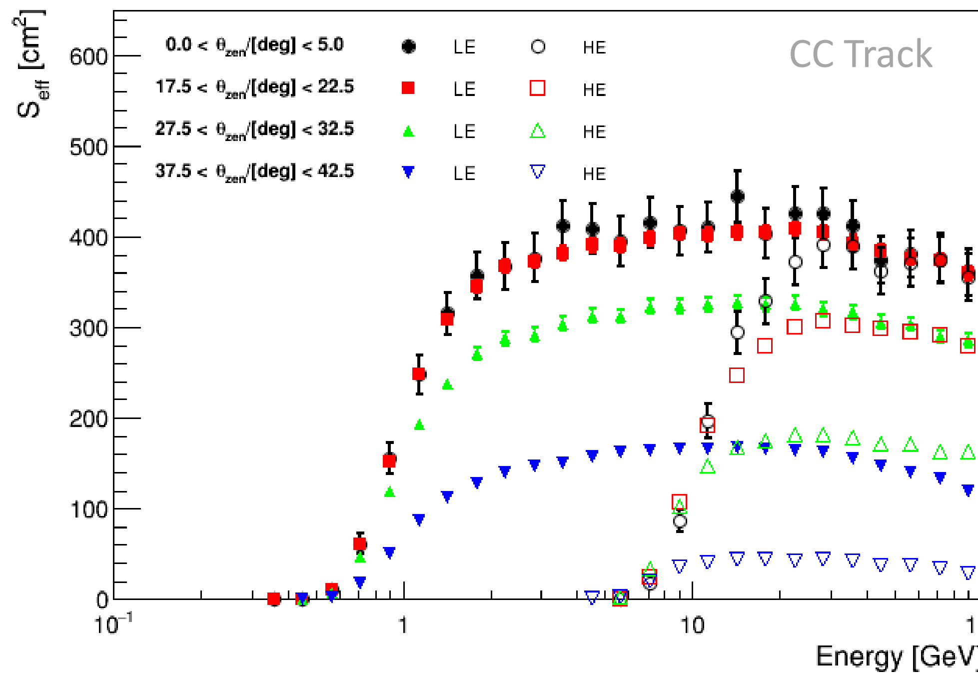

Mostly axially symmetric except for FOV cut

Effective area as a function of energy. Four representing zenith angle ranges are shown.

→ Talk by Fujita (25pK202-10)

CALET Collaboration

O. Adriani[25], Y. Akaike[2], K. Asano[7], Y. Asaoka[9,31], M.G. Bagliesi[29], G. Bigongiari[29], W.R. Binns[32], S. Bonechi[29], M. Bongi[25], P. Brogi[29], J.H. Buckley[32], N. Cannady[12], G. Castellini[25], C. Checchia[26], M.L. Cherry[12], G. Collazuol[26], V. Di Felice[28], K. Ebisawa[8], H. Fuke[8], G.A. de Nalfo [14], T.G. Guzik[12], T. Hams[3], M. Hareyama[23], N. Hasebe[31], K. Hibino[10], M. Ichimura[4], K. Ioka[34], W.Ishizaki[7], M.H. Israel[32], A. Javaid[12], K. Kasahara[31], J. Kataoka[31], R. Kataoka[16], Y. Katayose[33], C. Kato[22], Y.Kawakubo[1], N. Kawanaka[30], H. Kitamura[15], H.S. Krawczynski[32], J.F. Krizmanic[2], S. Kuramata[4], T. Lomtadze[27], P. Maestro[29], P.S. Marrocchesi[29], A.M. Messineo[27], J.W. Mitchell[14], S. Miyake[5], K. Mizutani[20], A.A. Moiseev[3], K. Mori[9,31], M. Mori[19], N. Mori[25], H.M. Motz[31], K. Munakata[22], H. Murakami[31], Y.E. Nakagawa[8], S. Nakahira[9], J. Nishimura[8], S. Okuno[10], J.F. Ormes[24], S. Ozawa[31], L. Pacini[25], F. Palma[28], P. Papini[25], A.V. Penacchioni[29], B.F. Rauch[32], S.B. Ricciarini[25], K. Sakai[3], T. Sakamoto[1], M. Sasaki[3], Y. Shimizu[10], A. Shiomi[17], R. Sparvoli[28], P. Spillantini[25], F. Stolzi[29], I. Takahashi[11], M. Takayanagi[8], M. Takita[7], T. Tamura[10], N. Tateyama[10], T. Terasawa[7], H. Tomida[8], S. Torii[9,31], Y. Tunesada[18], Y. Uchihori[15], S. Ueno[8], E. Vannuccini[25], J.P. Wefel[12], K. Yamaoka[13], S. Yanagita[6], A. Yoshida[1], K. Yoshida[21], and T. Yuda[7]

1) Aoyama Gakuin University, Japan
2) CRESST/NASA/GSFC and Universities Space Research Association, USA
3) CRESST/NASA/GSFC and University of Maryland, USA
4) Hirosaki University, Japan
5) Ibaraki National College of Technology, Japan
6) Ibaraki University, Japan
7) ICRR, University of Tokyo, Japan
8) ISAS/JAXA Japan
9) JAXA, Japan
10) Kanagawa University, Japan
11) Kavli IPMU, University of Tokyo, Japan
12) Louisiana State University, USA
13) Nagoya University, Japan
14) NASA/GSFC, USA
15) National Inst. of Radiological Sciences, Japan
16) National Institute of Polar Research, Japan
17) Nihon University, Japan
18) Osaka City University, Japan
19) Ritsumeikan University, Japan
20) Saitama University, Japan
21) Shibaura Institute of Technology, Japan
22) Shinshu University, Japan
23) St. Marianna University School of Medicine, Japan
24) University of Denver, USA
25) University of Florence, IFAC (CNR) and INFN, Italy
26) University of Padova and INFN, Italy
27) University of Pisa and INFN, Italy
28) University of Rome Tor Vergata and INFN, Italy
29) University of Siena and INFN, Italy
30) University of Tokyo, Japan
31) Waseda University, Japan
32) Washington University-St. Louis, USA
33) Yokohama National University, Japan
34) Yukawa Institute for Theoretical Physics, Kyoto University, Japan

CALET-CAL Detector

Fully active thick calorimeter ($30X_0$) optimized for electron spectrum measurements well into TeV region

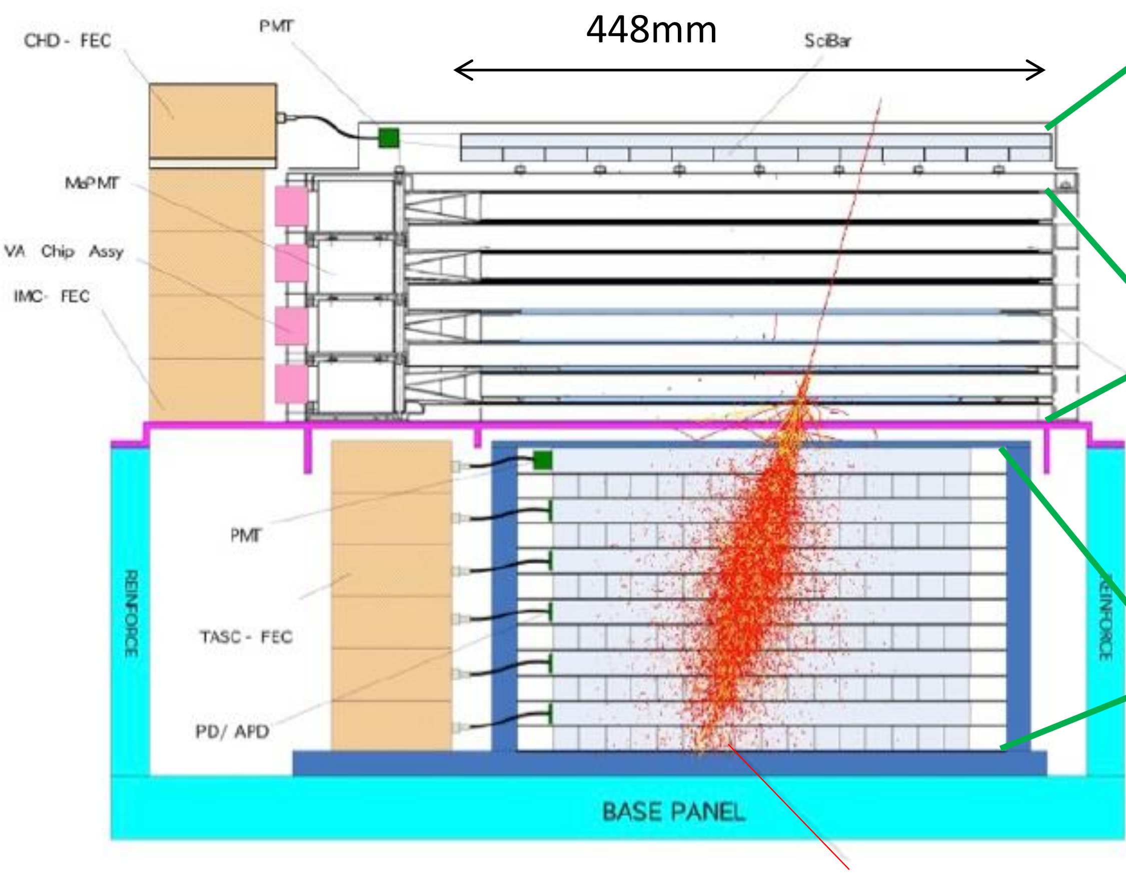

1TeV electron shower is fully contained in TASC

Charge Detector **CHD**

plastic scintillator hodoscope,
absolute charge measurement
(including charge zero)

Imaging Calorimeter **IMC**

SciFi + tungsten plate (3X0),
reconstruction of arrival direction and initial shower development

Total Absorption Calorimeter **TASC**

PWO hodoscope (27X0),
energy measurements and particle identification

Gamma Ray Event Selection

= Electron Selection Cut + Gamma-ray ID Cut w/ Lower Energy Extension

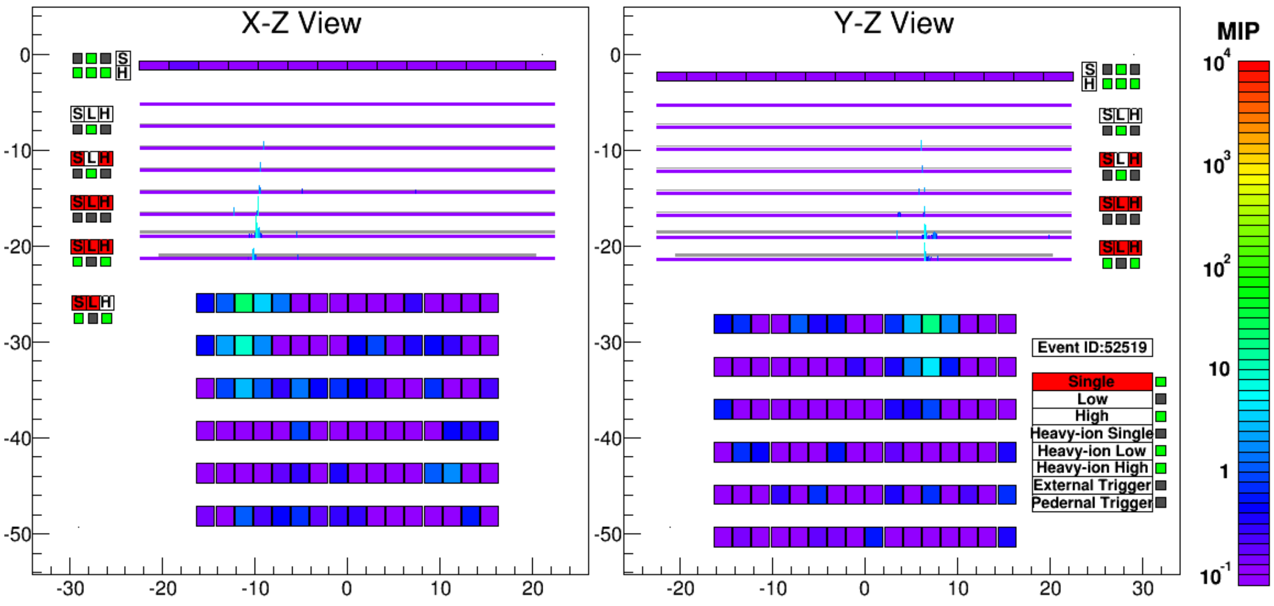

An example of gamma-ray event candidate in flight data (reconstructed primary energy ~5GeV)

1. Geometry Condition
   - CHD-Top to TASC 1st layer (2cm margin)
2. Pre selection
   - Offline trigger
   - Shower concentration
   - Shower starting point
3. Track quality cut
   - Track hits >2
   - matching w/ TASC
4. Electromagnetic shower selection
   - shower shape
5. Gamma-ray ID
   - CHD/IMC-veto (combination of loose cuts)
6. FOV cut

Gamma Ray Event Selection

= Electron Selection Cut + Gamma-ray ID Cut w/ Lower Energy Extension

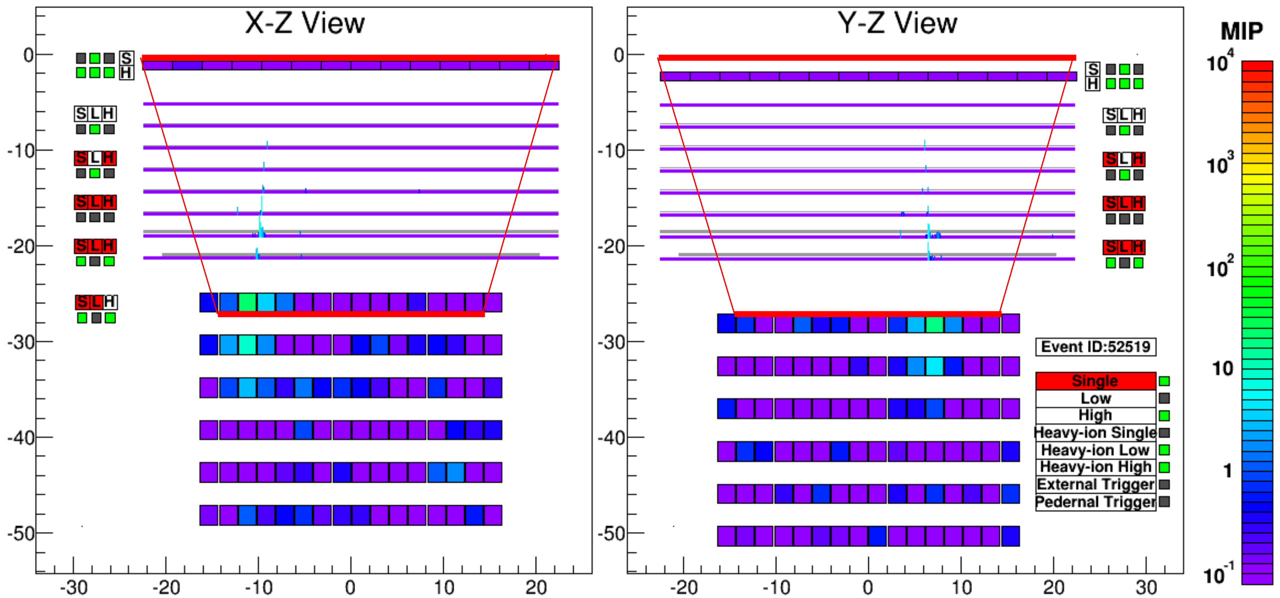

1. Geometry Condition
   - CHD-Top to TASC 1st layer (2cm margin)
2. Pre selection
   - Offline trigger
   - Shower concentration
   - Shower starting point
3. Track quality cut
   - Track hits >2
   - matching w/ TASC
4. Electromagnetic shower selection
   - shower shape
5. Gamma-ray ID
   - CHD/IMC-veto (combination of loose cuts)
6. FOV cut

To maximize the field of view (FOV), the requirements on acceptance condition was loosened as much as possible compared to electron analysis. However, penetration of CHD paddle by shower axis is required to ensure charge zero selection.

Gamma Ray Event Selection

= Electron Selection Cut + Gamma-ray ID Cut w/ Lower Energy Extension

"K-cut" $$K = \log_{10}(F_E) + \frac{1}{2}R_E$$

F_E : fractional energy deposit of TASC-Y6 relative to total TASC deposit

R_E : Second moment of lateral energy deposit distribution relative to shower axis [cm]

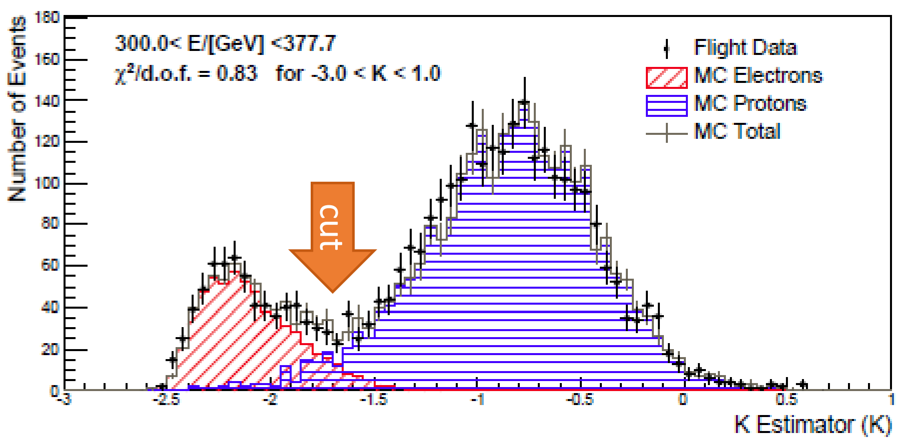

FIG. 2. An example of K-estimator distribution in the $300 < E < 378$ GeV bin. The reduced chi-square of the fit in the K-estimator range from -3 to 1 is 0.83.

O. Adriani et al., PRL 119, 181101 (2017) supplemental material

1. Geometry Condition
   - CHD-Top to TASC 1st layer (2cm margin)
2. Pre selection
   - Offline trigger
   - Shower concentration
   - Shower starting point
3. Track quality cut
   - Track hits >2
   - matching w/ TASC
4. Electromagnetic shower selection
   - shower shape
5. Gamma-ray ID
   - CHD/IMC-veto (combination of loose cuts)
6. FOV cut

Gamma Ray Event Selection

= Electron Selection Cut + Gamma-ray ID Cut w/ Lower Energy Extension

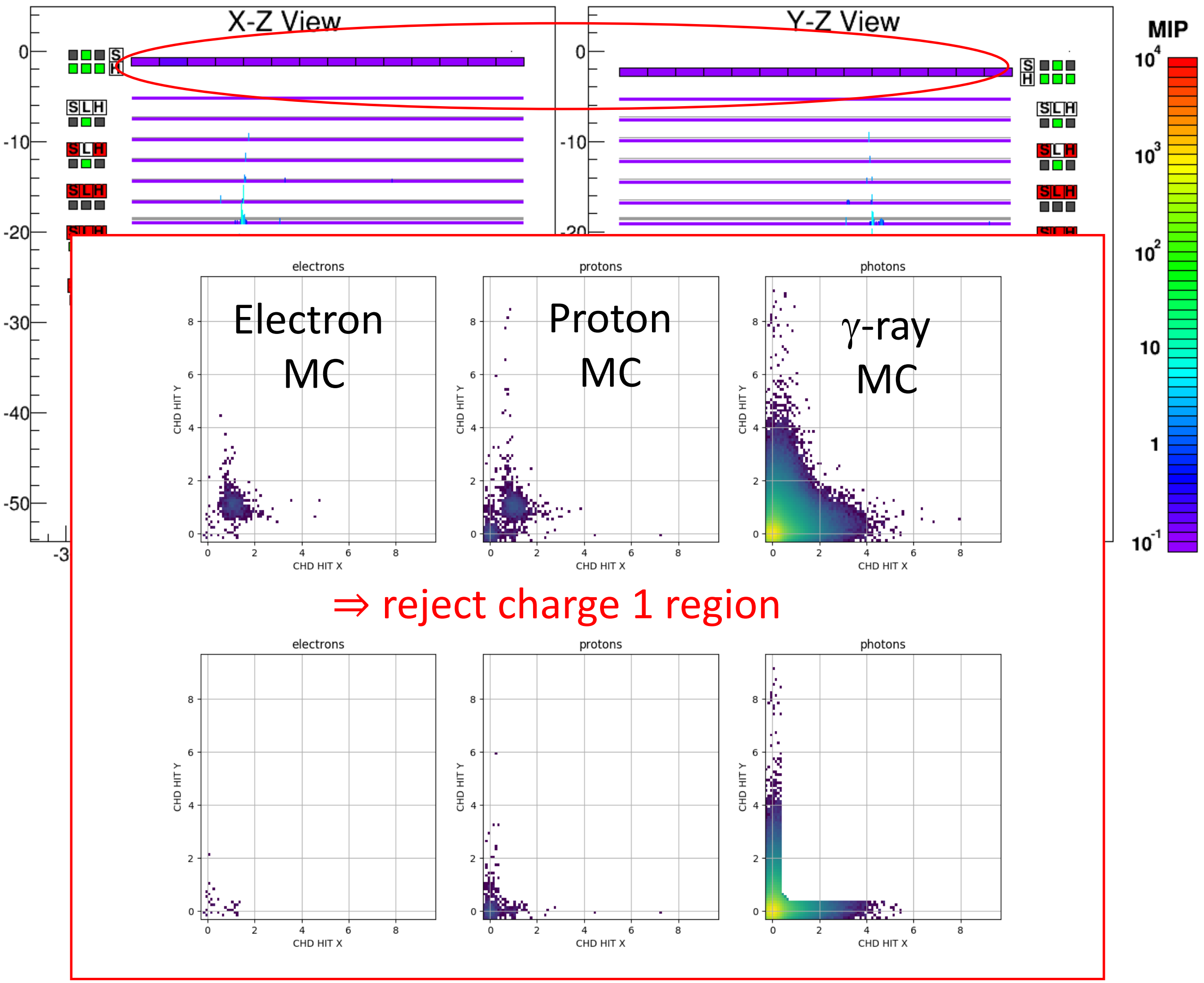

1. Geometry Condition
   - CHD-Top to TASC 1st layer (2cm margin)
2. Pre selection
   - Offline trigger
   - Shower concentration
   - Shower starting point
3. Track quality cut
   - Track hits >2
   - matching w/ TASC
4. Electromagnetic shower selection
   - shower shape
5. **Gamma-ray ID**
   - **CHD/IMC-veto (combination of loose cuts)**
6. FOV cut

Gamma Ray Event Selection

= Electron Selection Cut + Gamma-ray ID Cut w/ Lower Energy Extension

It was found that secondary gamma-ray produced in ISS structures are dominant source of background

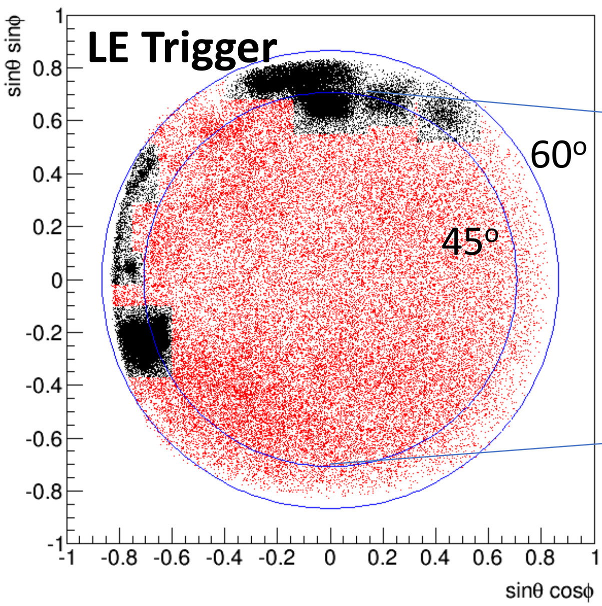

Gamma-ray candidates in CALET FOV

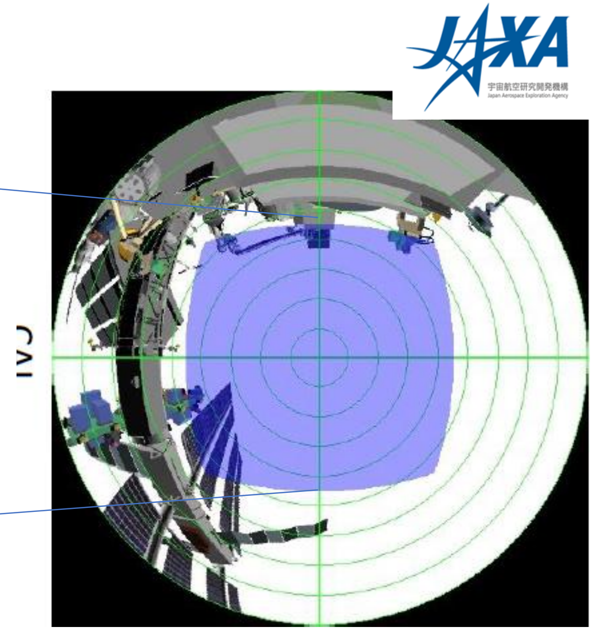

Fish-eye view of CALET FOV

By removing Black parts, it is possible to reject majority of such background. More sophisticated rejection method is under development.

1. Geometry Condition
   - CHD-Top to TASC 1st layer (2cm margin)
2. Pre selection
   - Offline trigger
   - Shower concentration
   - Shower starting point
3. Track quality cut
   - Track hits >2
   - matching w/ TASC
4. Electromagnetic shower selection
   - shower shape
5. Gamma-ray ID
   - CHD-veto
6. FOV cut

EM Track vs CC Track: Effective area

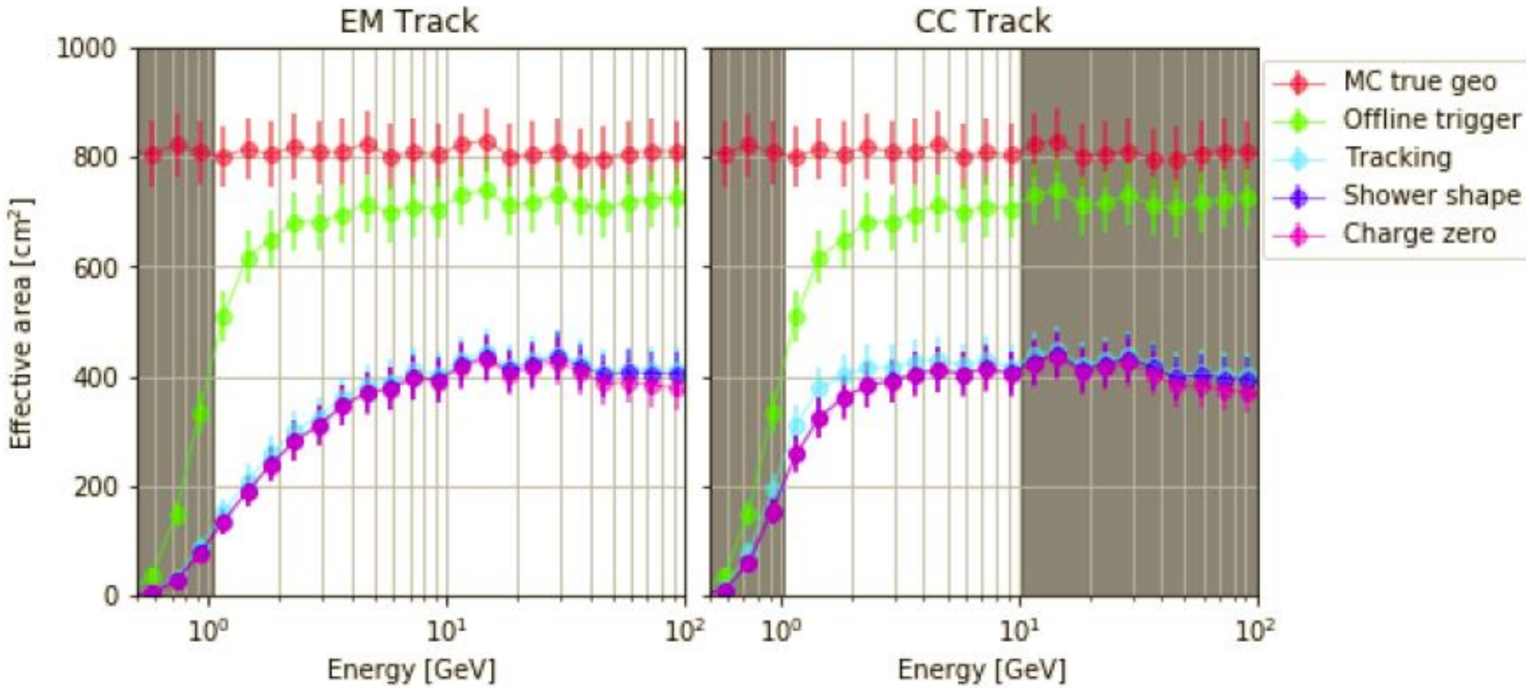

Figure 3. Effect of various selection cuts in zenith-pointing effective area. Grey shaded regions demonstrate the limits of applicability for each track due to background contamination with poor agreement between flight data and simulation.

EM Track vs CC Track : PSF

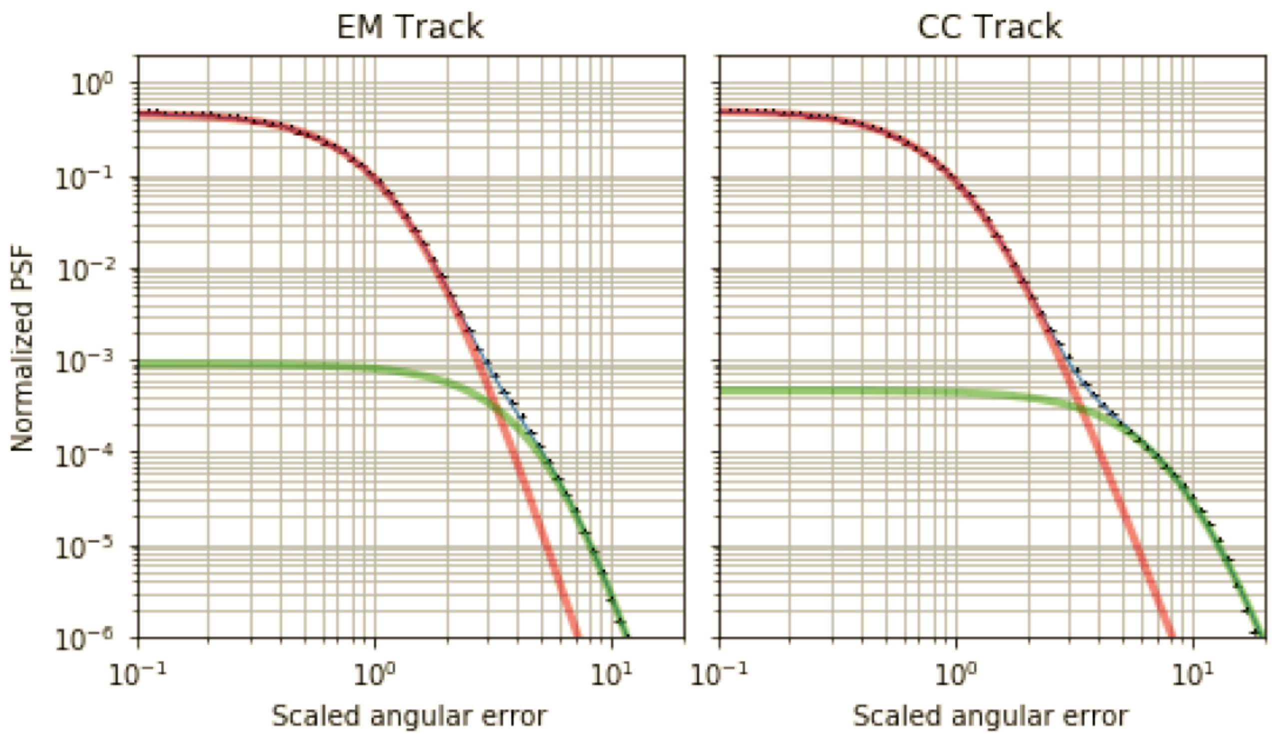

Figure 6. Composite PSF for EM and CC tracks. In each plot, the core contribution and tail contribution are represented by the red and green curves, respectively.

Point Source Spectra: Sensitivity Validation

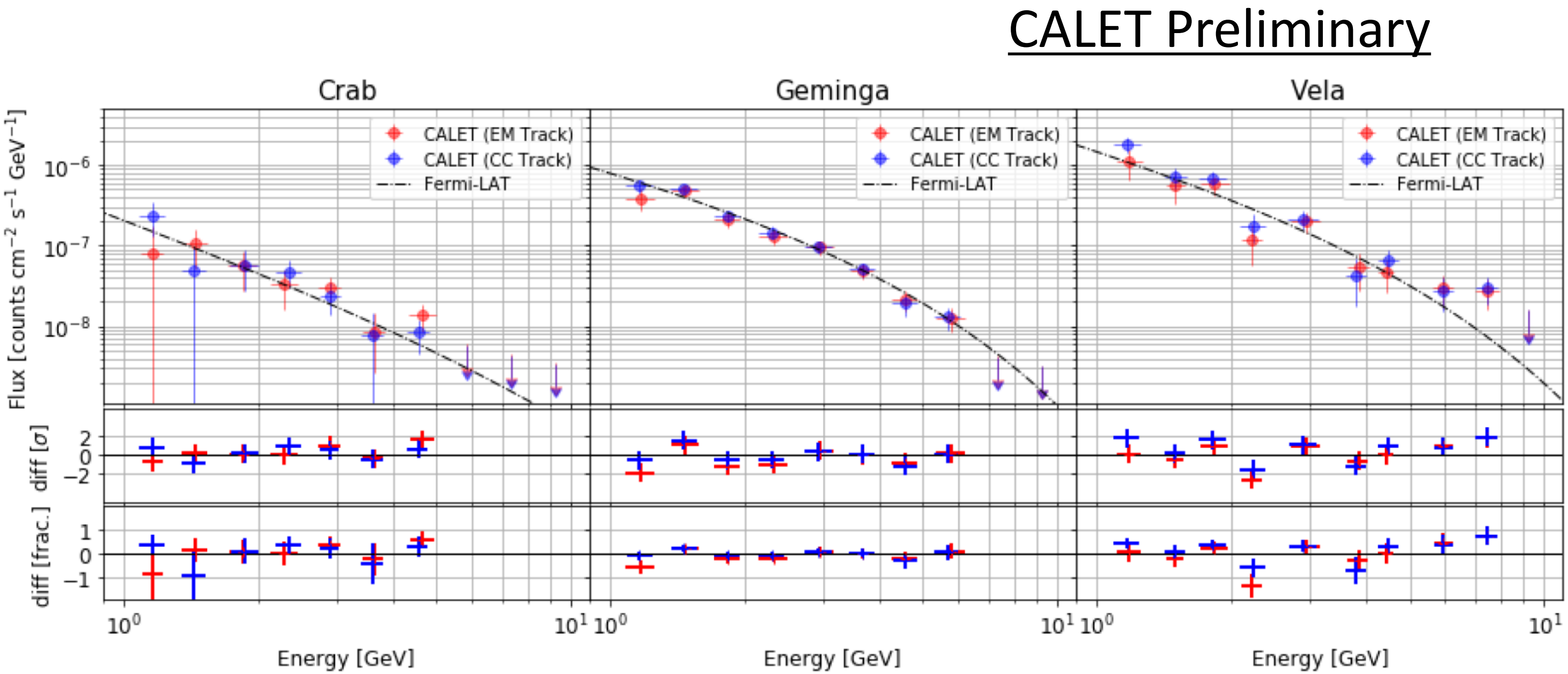

The observed point source spectra are well consistent with Fermi-LAT's parameterizations. Therefore, it was found that current selection criteria has a validated sensitivity and can be used to set limit on GW counterpart flux.

https://www.slac.stanford.edu/exp/glast/groups/canda/lat_Performance.htm

Fermi LAT performance

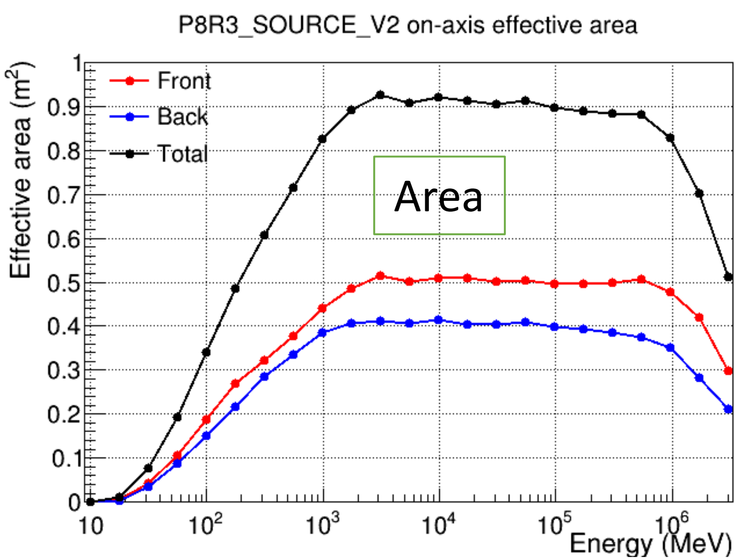

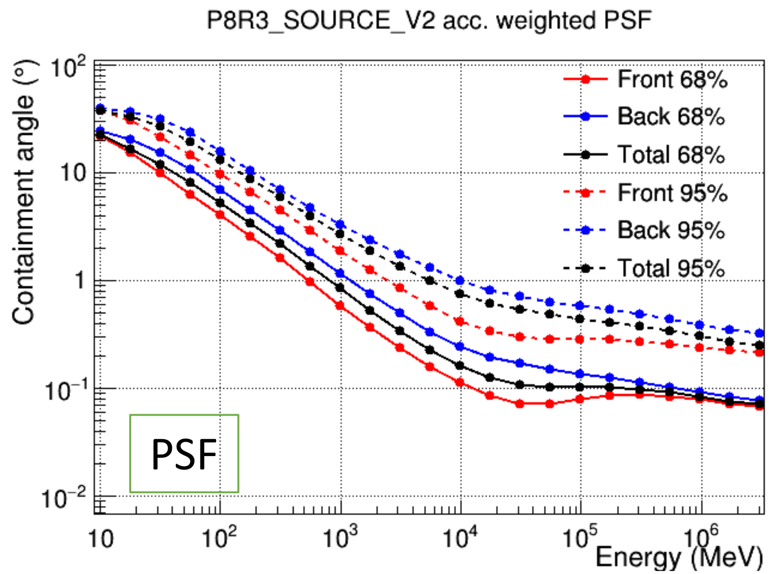

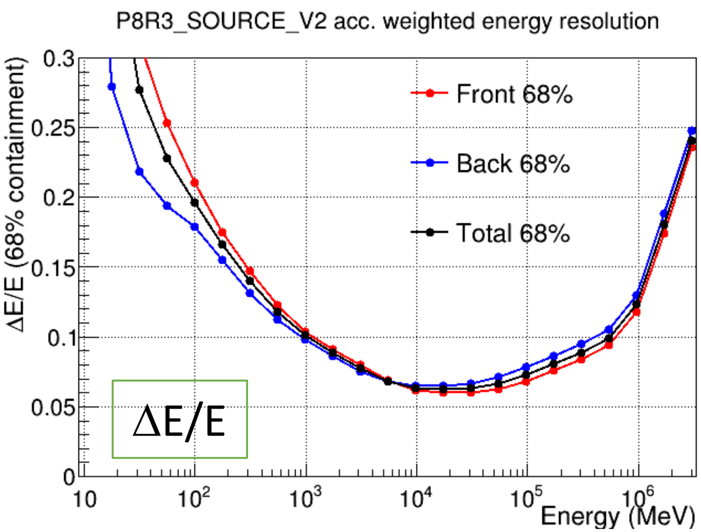

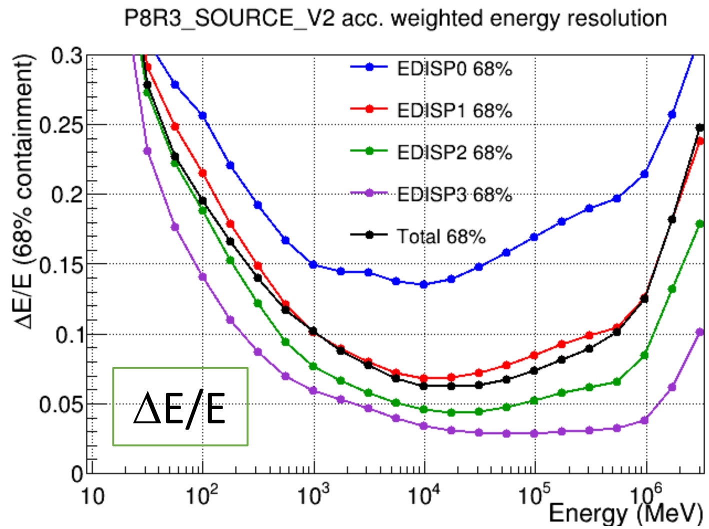

GRB analysis following a CGBM trigger: an example

GRB 180126A: triggered by CGBM at T_0=2018/1/26/ 2:16:38 UTC
$\rightarrow$ No gamma ray candidates within $T_0 \pm 60$s

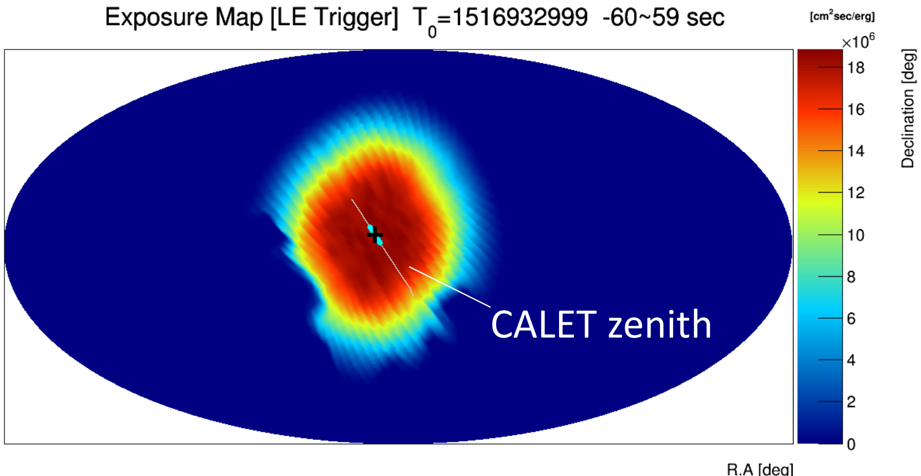

Exposure during 120s

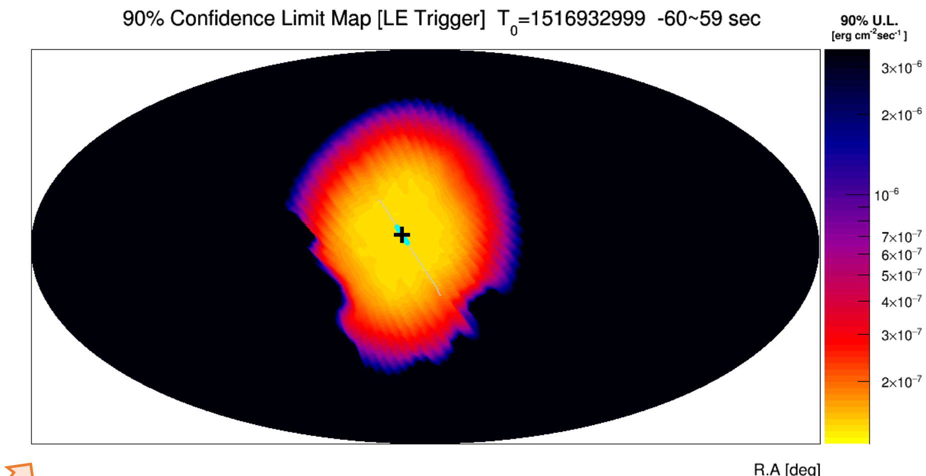

Upper limits on energy flux (0 event)

Upper limits are calculated assuming number of events N_0 corresponding to 90% C.L.

- 0 event $\rightarrow N_0 = 2.44$
- 1 event $\rightarrow N_0 = 4.36$
- 2 events, not a pair $\rightarrow N_0 = 4.38/0.68$

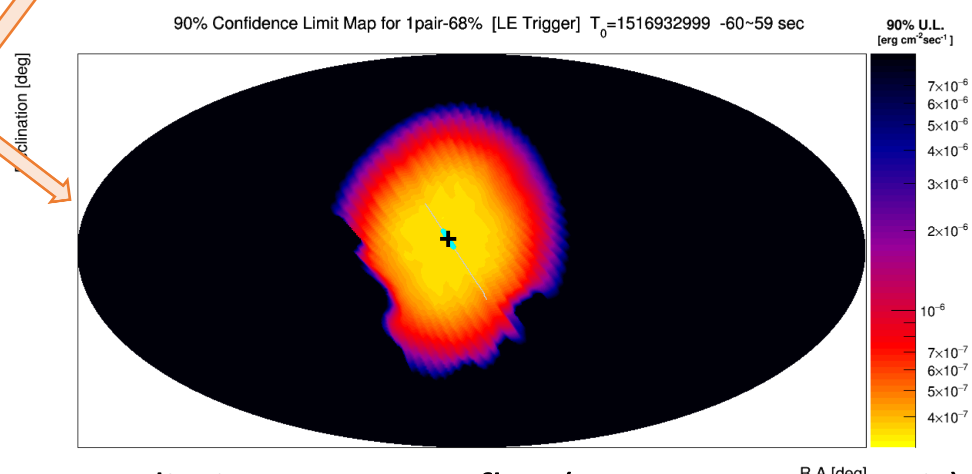

Upper limits on energy flux (2 events, not a pair)